universität wien

MASTERARBEIT / MASTER'S THESIS

Titel der Masterarbeit / Title of the Master's Thesis

„Actinides in Cryoconite Samples from an Alpine Glacier“

verfasst von / submitted by

Leo Johannes Krammer, BSc

angestrebter akademischer Grad / in partial fulfilment of the requirements for the degree of

Master of Science (MSc)

Wien, 2020 / Vienna 2020

Studienkennzahl lt. Studienblatt / degree programme code as it appears on the student record sheet:	UA 066 862
Studienrichtung lt. Studienblatt / degree programme as it appears on the student record sheet:	Masterstudium Chemie
Betreut von / Supervisor:	ao. Univ.-Prof. Mag. Dr. Gabriele Wallner

Declaration of Academic Integrity

I hereby declare that I have authored this thesis independently and that I have not used other than the declared sources/resources. I have explicitly indicated all material, which has been quoted either literally or by content from the used sources. Unless otherwise marked, illustrations, pictorial representations, and schemes are my own.

Date	Signature

Acknowledgement

First, I want to thank Prof. Dr. Gabriele Wallner (Institute of Inorganic Chemistry, University of Vienna) for entrusting me with this interesting topic, for the supervision of this thesis and the great support during the research.

I also want to thank Dr. Karin Hain, Michael Kern, and Florian Mozina from the VERA Institute for introducing me to AMS and their help during lab work.

Special thanks go to my family for always supporting me and making my academic studies possible. Also, I want to thank all my friends for the good times and fun we have together.

Finally, I want to thank my girlfriend Marlene for being at my side for eight years of my life now. Thank you for your love and always being there for me.

Table of Contents

1 Introduction

Radioactivity is omnipresent throughout the environment. It is caused by unstable, radioactive isotopes, which can be either of natural or artificial source. The former have been present on Earth since its formation and are incessantly produced by nuclear reactions between atoms in the atmosphere and cosmic rays. Some of them have very long half-lives (> 10^9 years) – comparable to the existence of our planet and the universe. Such radioactive isotopes are also called "primordial isotopes", indicating that they have existed since before formation of Earth. Some examples are the parent nuclides of the natural radioactive decay series – ^{235}U, ^{238}U and ^{232}Th.[1]

The latter derive from several anthropogenic sources, namely radioactive wastes of isotope laboratories, radioactive wastes of nuclear energy production and reprocessing technologies (e.g. introduction into the environment *via* accidents in nuclear power plants), and nuclear bombs (e.g. radioactive fallout) or experimental nuclear explosions. Longtime pollution originates from isotopes with long half-lives, e.g. ^{90}Sr, ^{137}Cs, ^{241}Am or Pu.[1]

Radioactive pollution deriving from fallout is increasing with altitude.[2] For example, the Austrian Alps have shown to be a hot spot for radioactive contamination by global fallout from the nuclear weapon tests, and especially by fallout from the Chernobyl reactor accident in 1986.[3] In fallout, the radionuclides are attached to aerosols or dust particles, which are then later deposited as airborne sediments on surfaces and glaciers. On glaciers they are suggested to be the parental material for the formation of cryoconites. This dark-colored matter is a specific type of supraglacial sediment, often found in so-called "cryoconite holes" caused by melting due to its thermal properties.[4] Since there is no dilution with other matrices, pollution substances like radioisotopes from global fallout are almost pure, resulting in the fact that the highest anthropogenic radionuclide concentrations in the environment are found in cryoconites.[3] Other contaminants (e.g. persistent organic pollutants[5,6]) can also be trapped in cryoconite holes. As the glacier melting is expected to increase in near future due to global warming, these contaminants, along with the radionuclides, might be released into downstream rivers[7], affecting both aquatic ecosystems and human health.[4]

2 Theoretical Background

2.1 Types of radioactive decay

There exist three basic decay modes: α-, β-, and γ-decay. In 1899, Ernest Rutherford found that radiation deriving from uranium consists of at least two types.[8] In his experiments, one type of radiation was easily absorbed by a thin layer of metal foil or paper and by convenience, he termed this type ***α*** radiation. In α-decay, an α particle is emitted, which basically is a $^4He^{2+}$-ion. Although this suggestion was immediately made, it was eventually proven by William Ramsey in 1903[1] and by Rutherford and Thomas Royds in 1908.[9] Alpha decay usually occurs in very heavy nuclides (> 106 u), such as uranium, thorium or radium. An example for the decay reaction is shown in Equation (Eq.) **(1)**.

$$^{238}_{92}U \rightarrow {}^{234}_{90}Th + {}^{4}_{2}He \qquad \textbf{(1)}$$

The second type of radiation discovered by Rutherford, ***β*** radiation, was of a more penetrative character, as it was able to pass through the investigated substances with far greater facility.[8] Beta decay materializes in three different ways: β^-, β^+ and electron capture. In β^--decay, a neutron-rich nuclide (e.g. a fission product in a nuclear reactor) stabilizes itself by converting a neutron into a proton, accompanied by the emission of an electron (e^- or β^-) – due to the principle of charge conservation – and an antineutrino ($\bar{\nu}_e$). An example for β^-decay is shown in Eq. **(2)**.

$$^{234}_{91}Pa \rightarrow {}^{234}_{92}U + e^- + \bar{\nu}_e \qquad \textbf{(2)}$$

Unstable, proton-rich nuclei (e.g. ^{68}Ga) undergo β^+-decay. In this case, a proton is converted into a neutron, followed by subsequent emission of a positron (e^+ or β^+) and a neutrino (ν_e). An example is given in Eq. **(3)**.

$$^{18}_{9}F \rightarrow {}^{18}_{8}O + e^+ + \nu_e \qquad \textbf{(3)}$$

The emitted positron may further be annihilated by an electron, which leads to the production of two anti-parallel gamma rays. This principle is used in a medical imaging technique called *positron emission tomography* (PET).[10]

Positron emission is often in competition with the third beta process, electron capture (EC). In EC, an electron from the inner electron shells – usually K or L shell – is absorbed by a proton-rich nucleus and a neutron is formed, accompanied by the emission of a neutrino. In addition, further emission of X-rays or Auger electrons can occur due to the creation of electron holes.

K-electron capture could be observed for the first time in 1937 by Luis Alvarez.[11] An example for an EC reaction is shown in Eq. **(4)**.

$$^{67}_{31}Ga + e^- \rightarrow ^{67}_{30}Zn + \nu_e \quad \textbf{(4)}$$

Potassium-40 is one of the few isotopes that can undergo all types of beta decay. The corresponding reactions are given in Eq. **(5)** to Eq. **(7)**.

$$^{40}_{19}K \rightarrow ^{40}_{20}Ca + e^- + \bar{\nu}_e \quad \textbf{(5)}$$

$$^{40}_{19}K \rightarrow ^{40}_{18}Ar + e^+ + \nu_e \quad \textbf{(6)}$$

$$^{40}_{19}K + e^- \rightarrow ^{40}_{18}Ar + \nu_e \quad \textbf{(7)}$$

The third of the three basic decay modes, γ-decay, does not result in a change in the number of nucleons. Gamma radiation usually occurs as a follow-up process of alpha or beta decay, when a daughter nucleus is in an excited state. The nucleus decays to a lower energy state by the emission of a high energy photon. The term 'γ ray' was also coined by Ernest Rutherford.[12] An example for gamma decay is given in Eq. **(8)** and Eq. **(9)**. ^{60}Co decays to ^{60}Ni, and the activated nickel nucleus emits two gamma rays, with 1.17 MeV (γ_1) and 1.33 MeV (γ_2) respectively (with 99.92 % probability).[13]

$$^{60}_{27}Co \rightarrow ^{60}_{28}Ni^* + e^- + \bar{\nu}_e \quad \textbf{(8)}$$

$$^{60}_{28}Ni^* \rightarrow ^{60}_{28}Ni + \gamma_1 + \gamma_2 \quad \textbf{(9)}$$

Like in electron capture, the nucleus can also interact with one of the orbital electrons through energy transfer, which is called *internal conversion* (IC). The electron will then be emitted from the atom, creating an electron hole in the shell. X-ray emission or other accompanying processes – as in EC – may then occur.[1] High energy electrons leaving the atom after IC should not be confused with β^- particles, as they are not emitted from the nucleus during the beta decay process.

Besides these three basic decay modes, other types of emission were gradually discovered. These include neutron emission[14], proton emission[15], spontaneous fission[16] and cluster decay[17].

2.2 Radioactive equilibria

Nuclides undergoing radioactive decay often form daughter nuclides, which are unstable as well. Their genetic relations may be written as follows:

$$nuclide\ 1 \rightarrow nuclide\ 2 \rightarrow nuclide\ 3 \quad \textbf{(10)}$$

Nuclide 1 is called mother nuclide of nuclide 2, which is called daughter nuclide of nuclide 1 and itself being the mother nuclide of nuclide 3. The net production rate for nuclide 2 is given by the decay rate of nuclide 1 minus the decay rate of nuclide 2.

$$\frac{dN_2}{dt} = -\frac{dN_1}{dt} - \lambda_2 N_2 = \lambda_1 N_1 - \lambda_2 N_2 \quad \textbf{(11)}$$

Substitution of N_1 by $N_{1,0}e^{-\lambda t}$ (with $N_{1,0}$ being the number of atoms of nuclide 1 at time 0) yields the following equation:

$$\frac{dN_2}{dt} + \lambda_2 N_2 - N_{1,0}e^{-\lambda t} = 0 \quad \textbf{(12)}$$

This is a first-order differential equation. Its solution is

$$N_2 = \frac{\lambda_1}{\lambda_2 - \lambda_1} N_{1,0}(e^{-\lambda_1 t} - e^{-\lambda_2 t}) + N_{2,0}e^{-\lambda_2 t} \quad \textbf{(13)}$$

$N_{2,0}$ represents the number of atoms of nuclide 2 at t = 0. By assuming that nuclides 1 and 2 are separated quantitatively at t = 0 the term $N_{2,0}$ equals zero and Eq. **(13)** can be simplified to

$$N_2 = \frac{\lambda_1}{\lambda_2 - \lambda_1} N_{1,0}(e^{-\lambda_1 t} - e^{-\lambda_2 t}) \quad \textbf{(14)}$$

Rearranging gives

$$N_2 = \frac{\lambda_1}{\lambda_2 - \lambda_1} N_1(1 - e^{-(\lambda_2 - \lambda_1)t}) \quad \textbf{(15)}$$

Equation **(15)** describes the radioactive equilibrium as a function of time after quantitative separation of the daughter nuclide from the mother nuclide. After a sufficiently long time, the exponential function in Eq. **(15)** will equal zero and a radioactive equilibrium is established. The decay constants λ can also be substituted by half-lives $t_{1/2}$.

$$N_2 = \frac{\lambda_1}{\lambda_2 - \lambda_1} N_1 = \frac{{t_{1/2}(2)}/{t_{1/2}(1)}}{\lambda_2 - {t_{1/2}(2)}/{t_{1/2}(1)}} N_1 \qquad \textbf{(16)}$$

The ratio of atom numbers N_2/N_1 and the activity ratio becomes constant when radioactive equilibrium is established. At this point, four different cases can be distinguished:

a) $t_{1/2}(1) \gg t_{1/2}(2)$
The half-life of nuclide 1 is much longer than the half-life of nuclide 2.

b) $t_{1/2}(1) > t_{1/2}(2)$
The half-life of nuclide 1 longer than the half-life of nuclide 2, but the decay of the mother nuclide 1 cannot be neglected.

c) $t_{1/2}(1) < t_{1/2}(2)$
The half-life of nuclide 1 is shorter than the half-life of nuclide 2. No radioactive equilibrium can be observed.

d) $t_{1/2}(1) \approx t_{1/2}(2)$
The half-lives of both nuclides 1 and 2 are similar.

Case a) is one of the most common ones and it is also called secular equilibrium. After considering that $t_{1/2}(1) \gg t_{1/2}(2)$ equals $\lambda_1 \ll \lambda_2$, Eq. **(15)** reduces to

$$N_2 = \frac{\lambda_1}{\lambda_2} N_1 (1 - e^{-\lambda_2 t}) \qquad \textbf{(17)}$$

Again, if mother nuclide 1 is separated quantitatively from daughter nuclide 2 at t = 0, radioactive equilibrium is established after $t \gg t_{1/2}(2)$ (in practice after about five half-lives of nuclide 2), and the activities of both nuclides are equal. This is also depicted in Figure 1. As an example, the secular equilibrium of mother nuclide ^{238}U ($t_{1/2}$ = 4.5 x 10^9 a) and daughter nuclide ^{234}Th ($t_{1/2}$ = 24.1 d; λ_2 = 2.9 x 10^{-2} d^{-1}) is depicted.

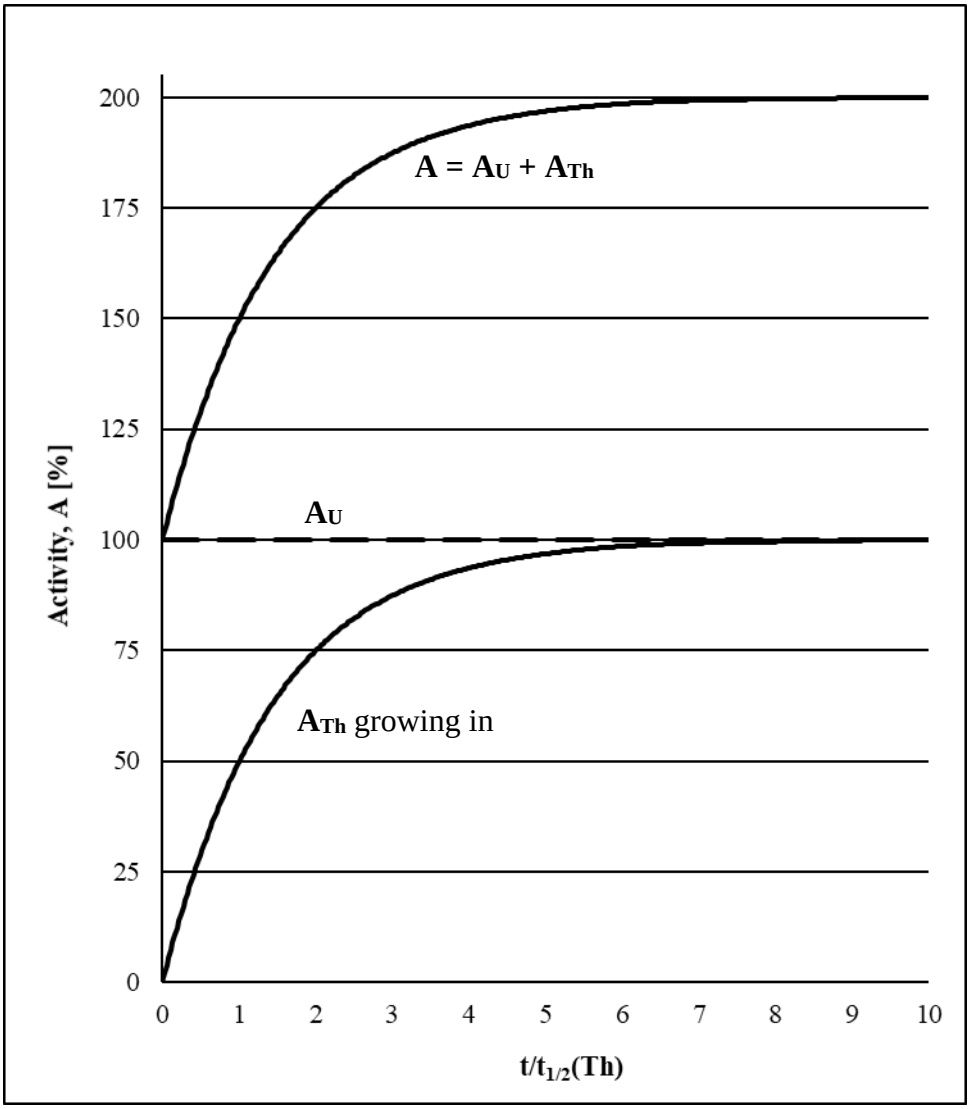

Figure 1: Secular equilibrium: Total activity A, and activities of mother nuclide (A_U) and daughter nuclide (A_{Th}) as a function of $t/t_{1/2}$(Th).

There are also technical applications that make use of the principle of secular radioactive equilibrium. For example, the shorter-lived, positron-emitting isotope ^{68}Ga ($t_{1/2}$ = 68 min) is used in diagnostic PET scans. It is steadily produced by electron capture from the longer-lived mother nuclide ^{68}Ge ($t_{1/2}$ = 271 d) in a ready-to-use generator, from which it can be easily eluted (as $^{68}GaCl_3$) with a few mL of dilute hydrochloric acid.[18]

2.3 Investigated radionuclides

2.3.1 Plutonium

The radioactive element plutonium (symbol: Pu; electron configuration: [Rn] $5f^6$ $7s^2$) belongs to the group of actinides. It is the element with the highest atomic number (Z = 94) to occur in nature (produced by cosmic radiation). However, the predominant fraction of Pu found in the

environment is of anthropogenic origin. Plutonium-238 was the first isotope to be isolated in 1940 (identified in 1941) by G. Seaborg, E. McMillan, J. W. Kennedy, and A. Wahl, *via* deuteron-bombardment of ^{238}U.[19,20] The corresponding reactions are given in Eq. **(18)** and **(19)**.

$$^{238}_{92}U + {}^{2}_{1}H \rightarrow {}^{238}_{93}Np + 2{}^{1}_{0}n \quad \textbf{(18)}$$

$$^{238}_{93}Np \rightarrow {}^{238}_{94}Pu + e^{-} + \bar{\nu}_e \quad \textbf{(19)}$$

The isotope with the highest longevity is ^{244}Pu, with a half-life of around 80 million years. Besides ^{238}Pu, the most widely produced isotopes are plutonium-239 and 240. ^{239}Pu is generated by the following reaction in Eq. **(20)**.

$$^{238}_{92}U(n,\gamma)^{239}_{92}U \xrightarrow{\beta^-} {}^{239}_{93}Np \xrightarrow{\beta^-} {}^{239}_{94}Pu \quad \textbf{(20)}$$

In all nuclear reactors operated with uranium as fuel, ^{239}Pu is produced by reaction **(20)**.[1] Furthermore, ^{239}Pu can be used as a reactor fuel itself because it is a fissile isotope. Unfortunately, plutonium-239 might also be used as the fissile material in nuclear weapons.

Plutonium dissolves well in acid – apart from concentrated nitric due to formation of a passivation layer – and exhibits several oxidation states (normally +3, +4, +5, +6, and +7) in aqueous solutions, with +4 being the most stable and +7 the rarest one. The standard electrode potentials of the several oxidation states show only marginal differences, thus Pu can co-exist simultaneously in several oxidation states. This fact complicates analytical radiochemistry of plutonium, as it also has an influence on separation processes.[21] Isotopes relevant for environmental samples are ^{238}Pu, ^{239}Pu, and ^{240}Pu. The main properties of the most important isotopes are summarized in Table 1.

Table 1: Characteristic properties of selected Pu-isotopes.[22,23]

Isotope	Half-life [a]	Decay mode	Energy α/β (intensity) [keV]
^{236}Pu	2.85	α, spontaneous fission (sf)	5768 (69 %)
^{238}Pu	87.7	α, sf	5499 (71 %)
^{239}Pu	24110	α, sf	5156 (73 %)
^{240}Pu	6564	α, sf	5168 (73 %)
^{241}Pu	14.4	β^-	20.8 (E_{max}) 5.23 (average)
^{242}Pu	3.73 x 10^5	α, sf	4.901 (78 %)
^{244}Pu	8.13 x 10^7	α, sf	4.589 (80 %)

The largest source for Pu in the environment were the atmospheric nuclear weapon tests in the 1950s and 1960s, with about 400 kCi $^{239+240}$Pu – which corresponds to ~ 15 x 10^{15} Bq (petabecquerel) or ~ 6.4 t ^{239}Pu – released into the atmosphere.[24] In general, the origin of Pu found in nature can be determined by the ^{240}Pu/^{239}Pu-ratio. Normally (e.g. in weapon grade plutonium), the ratio is around 0.05 to 0.1.[25] In a nuclear reactor, ^{239}Pu is produced as shown in Eq. **(20)**. ^{240}Pu is then produced from ^{239}Pu *via* neutron capture (see Eq. **(21)**).

$$^{239}_{94}Pu + {}^{1}_{0}n \rightarrow {}^{240}_{94}Pu + \gamma \qquad \textbf{(21)}$$

But this process needs higher energy (e.g. during the explosion of a nuclear weapon) or longer time in a reactor. In the Northern Hemisphere fallout, deriving from the nuclear weapon tests, the ^{240}Pu/^{239}Pu-ratio is shifted to a higher ratio of 0.18[25,26] and in the Chernobyl fallout (1st of May 1986), a value of 0.4 is found.[25] These two ratios are of the most concern for this thesis, since samples from a glacier in the Northern Limestone Alps are discussed.

2.3.2 Americium

Americium (symbol: Am; Z = 95; electron configuration: [Rn] $5f^7$ $7s^2$) is a radioactive, synthetic element, belonging to the transuranic elements. It was discovered by G. Seaborg, R. James, L. Morgan, and A. Ghiorso in 1946 as the result of bombardment of uranium with high-energy helium ions in a cyclotron, and was named after a continent, like its lanthanide homolog Europium.[27] The most interesting isotopes of americium are ^{241}Am and ^{243}Am. Their main properties are given in Table 2.

Table 2: Characteristic properties of selected Am-isotopes.[23]

Isotope	Half-life [a]	Decay mode	Energy (intensity) [keV]
^{241}Am	432.6	α, sf	5485 (85 %)
^{243}Am	7364	α, sf	5275 (87 %)

Nowadays americium-241 is produced from plutonium-239 *via* the reaction shown in Eq. **(22)**. After two neutron captures, ^{241}Pu decays *via* a β^--process to ^{241}Am.

$$^{239}_{94}Pu(n,\gamma)^{240}_{94}Pu(n,\gamma)^{241}_{94}Pu \xrightarrow{\beta^- (14.35\ a)} {}^{241}_{95}Am \qquad \textbf{(22)}$$

It was used in smoke detectors as a source of ionization. When smoke enters the ionization chamber, it disrupts the electrical conductivity, which is built up by the ionization of the surrounding air by the emitted α-particles, and the alarm is triggered.[28]

2.3.3 Neptunium

Neptunium (symbol: Np; Z = 93; electron configuration: [Rn] $5f^4\ 6d^1\ 7s^2$) is a radioactive metal and the first transuranic element. It was first discovered – after many failed attempts by various working groups – by E. McMillan and P. Abelson in 1940.[29] ^{237}Np is the most produced isotope because it is formed as a side product in nuclear power plants. The corresponding reaction is given in Eq. **(23)**. ^{237}U is produced from ^{235}U *via* double neutron capture, which then decays to ^{237}Np.

$$^{235}_{92}U \xrightarrow{2\,(n,\gamma)} {}^{237}_{92}U \xrightarrow{\beta^-} {}^{237}_{93}Np \qquad \textbf{(23)}$$

Neptunium-237 is also the eponym of the (4n + 1) decay series, also called "neptunium series", since it is the longest-lived element ($t_{1/2}$ = 2.14 x 10^6 a[23]) in this series.[30] The natural neptunium series is considered to be 'extinct' because all neptunium present at the time when Earth was formed – approx. 4.6 billion years ago – has already decayed. Nowadays the series exists again due to the synthetic production of starting nuclides, such as ^{241}Pu, ^{241}Am, and ^{237}Np. Neptunium is used in neutron-detection instruments, but its applications in general are scarce.[31]

2.3.4 Thorium and Uranium

Thorium (symbol: Th; Z = 90; electron configuration: [Rn] $6d^2$ $7s^2$) is a silvery, radioactive metal from the actinoid series. Berzelius discovered it in 1828 in a mineral known as thorite ($ThSiO_4$). In 1898, M. Curie in Paris and G. Schmidt in Münster, working independently, discovered the radioactive character of thorium.[32] The most relevant isotopes for environmental samples are ^{232}Th (> 99.98 % abundance) and ^{230}Th (< 0.02 % ab.). All other isotopes are only present in trace amounts. A small list of isotopes and their main properties is given in Table 3.

Table 3: Characteristic properties of selected Th-isotopes.[23]

Isotope	Half-life [a]	Decay mode	Energy α/β (intensity) [keV]
^{228}Th	1.91	α	5423 (73 %)
^{229}Th	7880	α	4845 (56 %)
^{230}Th	7.54×10^4	α	4687 (76 %)
^{231}Th	25.52 **h**	β^-	80.1 (40 %) 85.3 (32 %)
^{232}Th	1.4×10^{10}	α	4012 (78 %)

Thorium-232 belongs to the primordial nuclides, meaning it has existed in its current form since before the formation of earth. With a half-life of approx. 14 billion years[23], ^{232}Th even has a half-life slightly longer than the age of the universe (approx. 13.8×10^9 a)[33] and gave the 4n decay series ("thorium series") its common name.

Thorium oxide is used as a catalyst in the production of sulfuric acid and in the conversion of ammonia to nitric acid. Thorium metal is used in fabricating portable gas lamps, as filament wire, in crucibles, and as breeder reactor fuel. When used as reactor fuel, ^{232}Th absorbs some of the thermal neutrons and becomes ^{233}U, which is an even more efficient reactor fuel than ^{235}U or plutonium.[34]

Uranium (symbol: U; Z = 92; electron configuration: [Rn] $5f^3$ $6d^1$ $7s^2$) is a silvery, radioactive, carcinogenic, and toxic (causes kidney damage) metal, occurring naturally in minerals (e.g. pitchblende). It was discovered in 1789 by Martin Klaproth, a German chemist, and was first isolated by Eugène Peligot, a French chemist, in 1841.[35] While the most abundant isotope, ^{238}U (> 99.2 %[23]), has its applications – as depleted uranium (< 0.3 % ^{235}U) – in the military sector (e.g. armor plating, armor-piercing projectiles) or civilian sector (e.g. radiation shielding, counterweights in aircraft), the isotope ^{235}U (~ 0.7 % abundance[23]) is used as main fuel in

nuclear power reactors[35], after enrichment to 3 – 5 %. A small list of the most relevant uranium isotopes for environmental samples and their main properties is given in Table 4.

Table 4: Characteristic properties of selected U-isotopes.[23]

Isotope	Half-life [a]	Decay mode	Energy (intensity) [keV]
^{234}U	2.46 x 10^5	α, sf	4774 (71 %)
^{235}U	7.04 x 10^8	α, sf	4395 (58 %)
^{236}U	2.34 x 107	α, sf	4494 (74 %)
^{238}U	4.47 x 10^9	α, sf	4198 (79 %)

2.4 Cryoconites

The name *cryoconite* derives from the ancient Greek words *krýos (cold, frost)* and *konía (powder, dust)*. They are formed by accumulation of mineral and organic dust together with microorganisms. Cryoconite particles cover the surface of glaciers, thus giving them their "dirty" look.[36] Due to the lowered albedo, more solar energy is absorbed and melting of the ice starts around cryoconite accumulations, initiating the formation of so-called cryoconite holes. These holes are of a cylindrical shape and can be several inches deep.[37]

Cryoconite granules (also see Figure 2) consist of mineral particles, organic matter, and several types of microbes (e.g. bacteria, algae). The spherical shape of the granules is maintained by filamentous cyanobacteria, which cover the surface (depicted in Figure 2) and trap mineral particles inside them.[38]

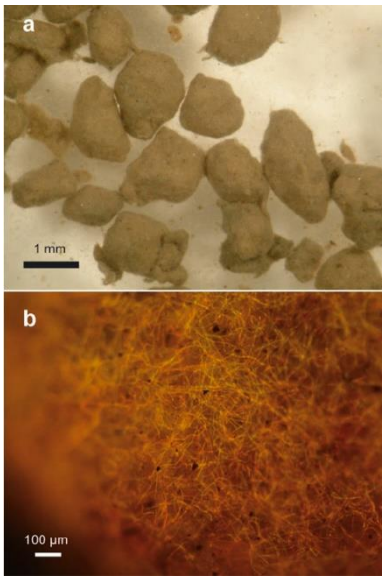

Figure 2: (a) Cryoconite granules under microscopic view; (b) fluorescent, filamentous cyanobacteria covering the granule surface (b) (Picture taken from Ref. [38]).

The color of the cryoconite granules varies between collection sites.[38] One assumes that the light absorption ability derives from humic substances, which are highly polymerized, organic compounds of residues remaining after the bacterial decomposition of organic matter.[39] These heteropolycondensates contain numerous conjugated double bonds (e.g. benzene rings), which absorb a wide range in the visible light spectrum.[40] Biological (e.g. cryoconite microbiome composition) or chemical conditions (e.g. pH value) may have an influence on the formation of humic substances in cryoconite granules, thus altering their content and color.[38]

2.4.1 Radionuclides in cryoconites

When released into the atmosphere (e.g. after nuclear accidents), radionuclides adsorb onto aerosols or dust particles and will then be deposited as fallout on all kinds of surfaces. On glaciers, these mineral or aerosol particles (containing radionuclides), together with microorganisms, will form cryoconite granules.[41] As no dilution with other environmental substances (e.g. soil) can occur, concentrations of radionuclides found in cryoconites are exceptionally high.[42]

Different working groups have been studying the radionuclide concentrations in cryoconites from different glaciers so far. Tieber and co-workers investigated the accumulation of radionuclides in cryoconites found on the alpine glaciers of Austria.[42] They identified two different populations of cryoconites: an older group, where values from nuclear weapon fallout prevail, and a younger group, dominated by Chernobyl fallout. The exact locations of the sampling sites are depicted in Figure 3.

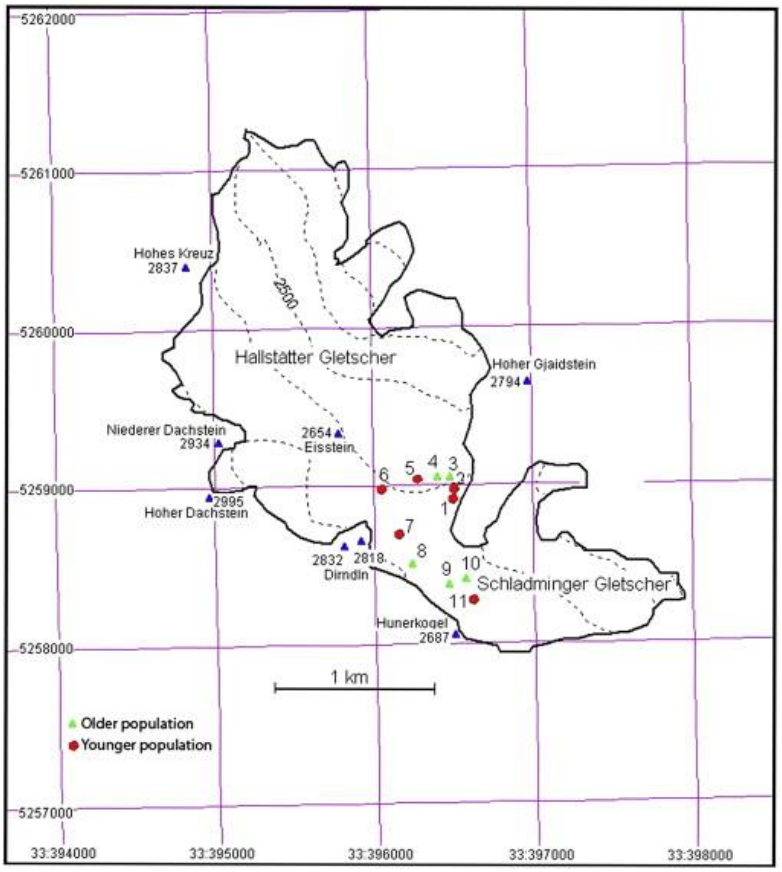

Figure 3: Locations of sample points on the Hallstätter and Schladminger glacier in the Northern Limestone Alps, Austria, by Tieber *et al.* (Picture taken from Ref. [42]).

The following anthropogenic radionuclides were identified in all samples by either gamma or alpha spectrometry: ^{241}Am, ^{207}Bi, ^{60}Co, ^{134}Cs, ^{137}Cs, ^{154}Eu, ^{238}Pu, $^{239+240}$Pu, ^{125}Sb, and ^{90}Sr. Apart from one sample, the activity concentrations of anthropogenic radionuclides exceeded the values usually found in common, environmental samples. In addition to this fact, the other main findings of the study were:

- A change of Sr/Cs and Sr/Pu ratios, compared to the initial fallout ratios, suggests strontium depletion over time.
- Isotopic ratios of cesium (^{134}Cs/^{137}Cs) and plutonium (^{238}Pu/$^{239+240}$Pu) were used to trace mixing processes of global (deriving from nuclear weapons) and Chernobyl fallout. The mixing has different causes, for example the perpetual addition of matter (e.g. dust) to a non-isolated cryoconite or the merging and subsequent mixing of two cryoconite pockets by melting of an ice layer, previously separating the two pockets.

Anthropogenic radionuclides – along with non-radioactive heavy metals – accumulated in cryoconites, found on an arctic glacier, were investigated by Łokas and co-workers in 2016.[41] They focused on the determination of activity concentrations of ^{137}Cs, ^{238}Pu, $^{239+240}$Pu, ^{90}Sr,

and natural radionuclide ^{210}Pb in cryoconites from Hans glacier, located in the Svalbard archipelago. The exact location of their study area and sampling sites is depicted in Figure 4.

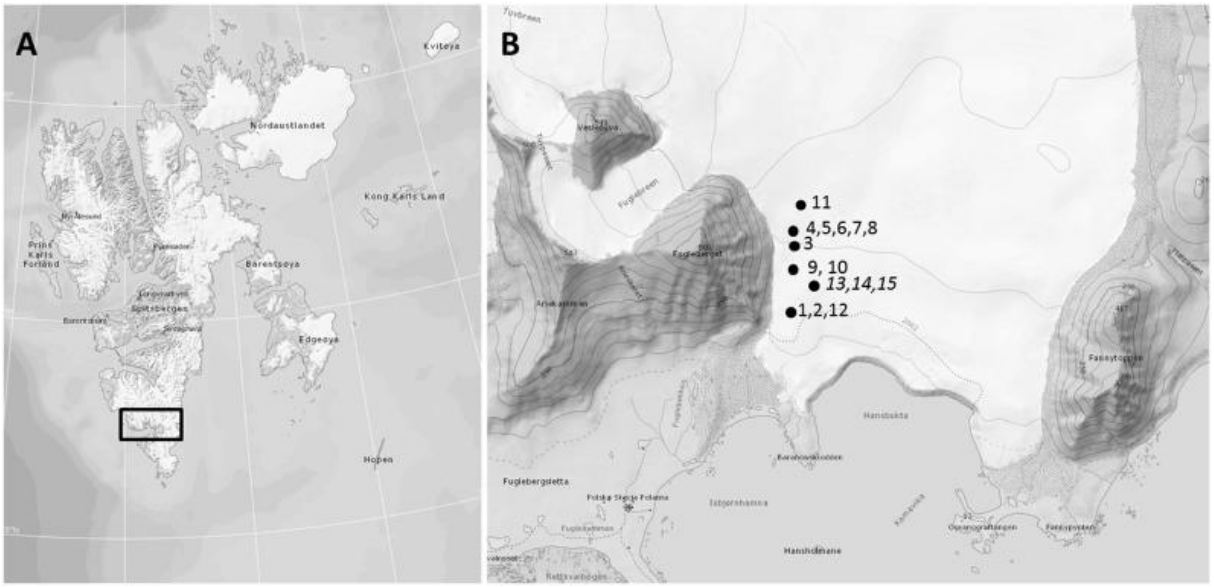

Figure 4: Locations of sample points on the Hans glacier in the Svalbard archipelago, Norway, by Łokas *et al.* (Picture taken from Ref. [41]).

Łokas *et al.* stated that the activity concentrations of cesium-137, lead-210, and the plutonium isotopes in the studied cryoconites exceeded values observed in Arctic peats, vegetation and organic soils. However, observed concentrations were lower than in Alpine cryoconites (e.g. Tieber *et al.*[42]), which can be explained by the reduced influence of global fallout (highest at 30 to 60° North) and the additional input of anthropogenic radionuclides by the Chernobyl accident in regions closer to Central Europe. Like Tieber and co-workers, Łokas *et al.* were also able to determine a mixing process of global and Chernobyl fallout based on ^{134}Cs/^{137}Cs and ^{238}Pu/$^{239+240}$Pu ratios.

3 Aim of this Thesis

Analysis of actinides in environmental samples, like cryoconites, might often be a tricky task, as some elements have a special behavior during sample preparation and the results (e.g. activity concentrations) may vary over a wide range. For example, plutonium with its several oxidation states (see also Chapter 3.2.1) causes problems from time to time, if it is not converted to a single oxidation state before chromatographic separation.

In order to confirm and reproduce previous results from analyses of cryoconite samples (*Cryo. 1, Cryo. 3, Cryo. 7, Cryo. 9*) from the Austrian Alps[42,43], this thesis was carried out, mainly dealing with the analysis of plutonium and americium in the mentioned cryoconite samples. A new approach to sample preparation is adopted due to discrepancies in the two previous analyses of the above stated cryoconite samples. When using sample material in a range of 0.5 to 1 g, alpha spectrometry data obtained by M. Bartmann[43] was in good agreement with the values reported by Tieber and co-workers (2.5 to 3.5 g sample material)[42]. However, AMS measurements required less sample material (~ 0.2 g) because of possible contamination and excess of plutonium. This resulted in large deviations from the values reported by Tieber *et al*., possibly due to either inhomogeneity of the samples ('hot particles') or loss of radioactive material in insoluble sample material during leaching.

In order to deal with this problem, thermal fusion (allowing complete digestion of the sample material, especially when small amounts are used) and a slightly altered ion exchange procedure should be applied for sample preparation and the effects on the results should be discussed. Furthermore, the altered ion exchange procedure should allow the preparation of a separate neptunium-fraction, which should then be analyzed by accelerator mass spectrometry.

4 Experimental Section

4.1 Sample Preparation

The Hallstätter glacier (Upper Austria) and the Schladminger glacier (Upper Austria) were sampled by Tieber and co-workers[42] in October 2006 (see also Section 2.4.1). The samples were then dried at 105 °C until they exhibited constant weight.

In order to achieve almost complete decomposition of the samples, thermal fusion with sodium carbonate turned out to be the method of choice. For this purpose, a sample preparation procedure from Becker *et al.*[44] was adapted to the cryoconite sample requirements. A homogenous mixture of the powdered sample (~ 100 mg) and sodium carbonate in ratio of 1/6 (w/w) was prepared. Fusion was then performed in a muffle furnace at 1000 °C using a Pt-crucible for 10 min, followed by subsequent cooling to room temperature. The decomposed mixture was then dissolved using 7.2 M HNO_3 and 10 M HCl. Spikes (^{243}Am, ^{242}Pu, ^{232}U; 10 µl each; activities are given in Table 5) – if needed – were added either before thermal fusion or after dissolving the decomposed mixture in acids. The influence of the time of the addition on the activity-results is discussed in Chapter 5.1.

Table 5: Activity concentrations for added spikes. ^{232}U-activity is decay-corrected for each day of α-spectrometry measurement.

Spike	**Activity concentration** [mBq/10 µL]
^{243}Am	46.3
^{242}Pu	14.4
^{232}U	17.7 (January 15, 2016)

^{242}Pu-spikes was added for quantitative analysis of $^{239+240}$Pu and ^{238}Pu, ^{243}Am-spike was added for ^{241}Am-analysis. ^{232}U-spike was added for the analysis of ^{234}U, ^{238}U and the Th-yield. As ^{232}U is in secular equilibrium with ^{228}Th (for explanation, see Chapter 2.2), the chemical yield of the thorium analysis can be determined by comparing the natural and altered ^{228}Th/^{232}Th-ratios. Analysis of Uranium was also achieved by using the ^{232}U-spike (see Chapter 4.2.5). No spikes were added for samples that were later analyzed by accelerator mass spectrometry (AMS).

The suspension was centrifuged (4000 rpm, 5 min) and the supernatant liquid was transferred into a beaker. The residue was again dissolved using H_2O dest. and subsequent dropwise addition of 40 w% HF. The solution was again centrifuged, and the supernatant liquid was combined with the other solution. Any undissolved material left was negligible (< 1 w%).

The combined solutions were then evaporated to dryness, followed by triple evaporation with 5 ml HNO_3 conc. to achieve full decomposition of fluorides, that may cause troubles in the separation process. The residue was dissolved in 10 ml 1 M HNO_3 and 100 mg $(NH_4)_2Fe(SO_4)_2 \cdot 6H_2O$ (Mohr's salt), 10 ml HNO_3 conc. and 0.5 g $NaNO_2$ were added in that order. $NaNO_2$ is used for the oxidation of Pu(III) – that is formed after the addition of Mohr's salt – to Pu(IV). The solution was then heated on a hot plate until formation of NO_x ceased. After cooling to room temperature, the solution was ready-to-use for ion exchange chromatography.

4.2 Chemical Separation and Practical Procedure

A general, schematic overview of the sample treatment for analysis of americium, thorium, plutonium and neptunium is shown in Figure 5.

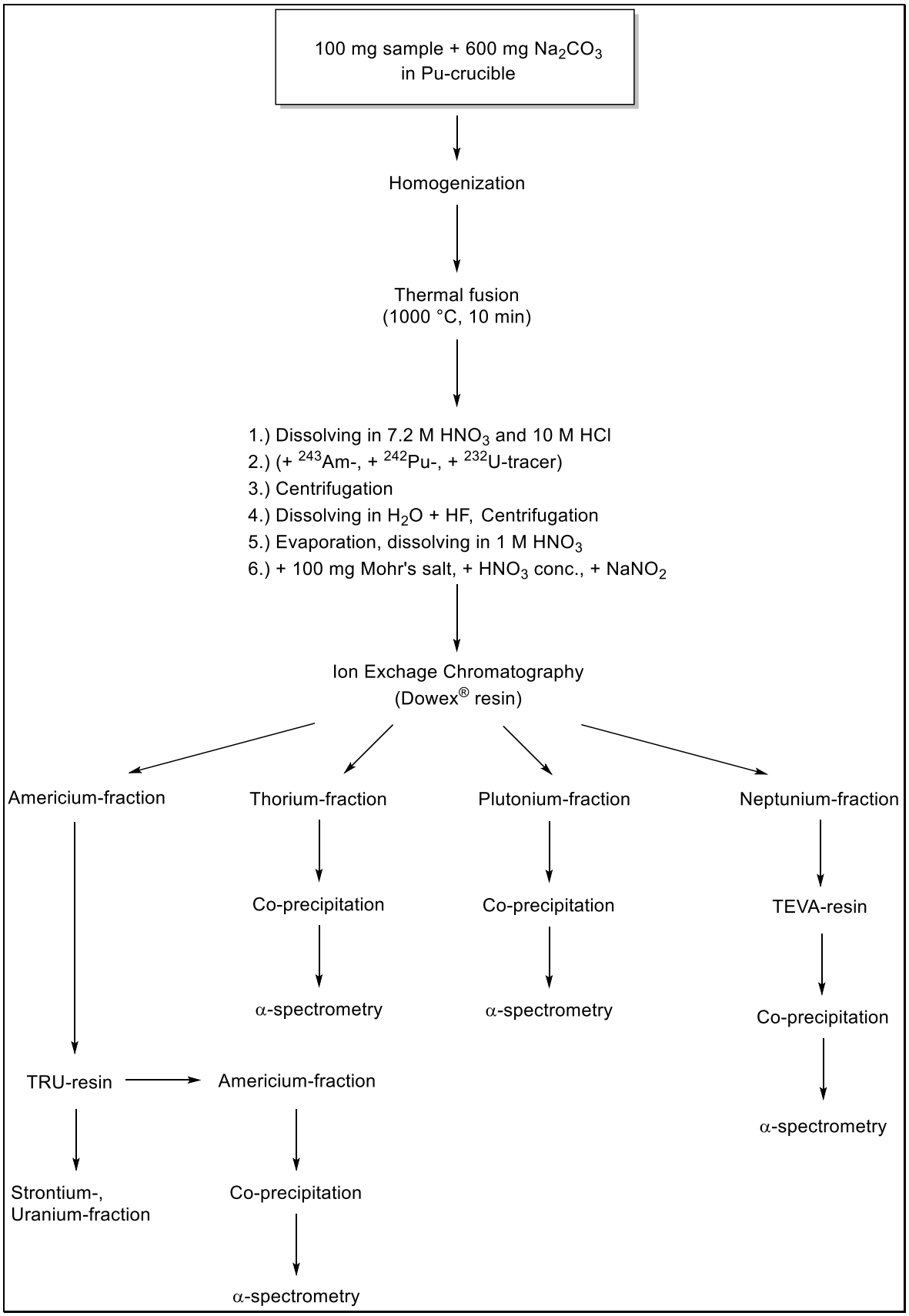

Figure 5: Schematic overview of sample treatment for alpha spectrometry of Am, Th, Pu and Np (sample preparation to alpha spectrometry).

The radiochemical separation *via* ion exchange chromatography was performed according to a procedure from Mietelski *et al*.[45] A first, rough separation of actinides was conducted *via* anion exchange chromatography using a DOWEX® 1X8 (8 % cross-linkage) chloride form resin with a particle size of 100-200 mesh.[46] The chemical structure is shown in Figure 6.

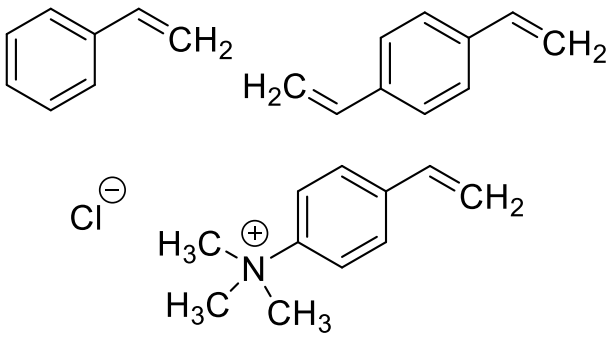

Figure 6: Chemical structure of the DOWEX® (chloride form) anion exchange resin.[47]

For this purpose, a column (Ø = 1.3 cm, filling level: 6.5 cm) with Dowex® resin – which had been soaked in distilled water and subsequently conditioned with 7.2 M HNO_3 – was prepared. After washing with 7.2 M HNO_3, the sample solution was loaded on the column, followed by rinsing of the beaker with 15 mL 7.2 M HNO_3 and a further column washing step with 15 mL 7.2 M HNO_3. The eluates of the loading and washing solutions were combined and used for the separation of americium (see Chapter 4.2.1). Thorium was then eluted with 40 mL 10 M HCl and the solution was stored for further analysis (see Chapter 4.2.2). The column was then washed with 50 mL of a solution of 0.1 M NH_4I in 9 M HCl to elute plutonium. Further treatment of this solution is depicted in Chapter 4.2.3. In a final washing step, neptunium was eluted with 40 mL 0.1 M HCl + 0.1 M HF.

4.2.1 Americium-fraction

The combined, Am-containing solutions were evaporated to dryness on a hot plate and the residue was dissolved in 300 mL 0.1 M HNO_3. 10 g $H_2C_2O_4 \cdot 2\,H_2O$ (20 g for analysis of reference material; see Section 4.2.7) and 10 mL 0.2 M $Ca(NO_3)_2$-solution (20 mL for analysis of reference material; see Section 4.2.7) were added and the solution was subsequently heated to 90 °C. The pH was adjusted to 4.5 with 25 w% NH_3-solution. A colorless precipitate formed, which was separated *via* centrifugation after cooling to room temperature. The precipitate was then evaporated three times with 5 mL HNO_3 conc. + 2 mL 30 w% H_2O_2 and dissolved in 20 mL 2 M HNO_3. A few granules of NH_4SCN and a pinch of ascorbic acid were added to the solution to reduce Fe(III) to Fe(II), which was essential for the following separation step.

Separation of americium from strontium and uranium was then conducted *via* column chromatography by using a TrisKem® TRU resin. "**TRU**" stands for "**TR**ans**U**ranian elements" and it consists of octylphenyl-*N*,*N*-diisobutyl carbamoylphosphine oxide (CMPO; structure given in Figure 7). Transuranian elements (including americium) have shown to have a high affinity to the resin at increasing HNO_3 concentrations. Fe(III) should not be present in the loading solution, as it is able to interfere with the Am-uptake. Therefore, it must be reduced to Fe(II), which is not retained on the resin at all.[48]

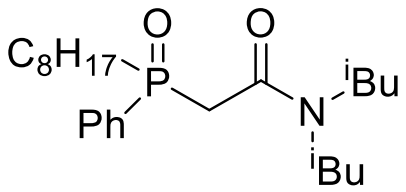

Figure 7: Octylphenyl-*N*,*N*-diisobutyl carbamoylphosphine oxide (CMPO)

The Fe-oxidation state adjusted Am-solution was loaded on the TRU-column (Ø = 0.9 cm, filling level: 4 cm; conditioned with 2 M HNO_3) and the beaker, followed by the column were washed with 5 mL 2 M HNO_3 respectively to eluate strontium. The column was then washed with 4 mL 9 M HCl to elute uranium. Americium was finally eluted with 15 mL 4 M HCl. The Am-solution was evaporated to dryness and the residue was evaporated three times with 5 mL HNO_3 conc. + 2 mL 30 w% H_2O_2. The resulting residue was then dissolved in 5 mL 1 M HNO_3 and the solution was transferred into a plastic test tube. 100 µL 0.5 mg/mL Nd^{3+}-solution were added and americium was co-precipitated with NdF_3 by the addition of 0.5 mL 40 w% HF. After waiting for 30 min, the solution was treated with ultrasound in a water bath for 1 min and was subsequently filtered through a cellulose nitrate membrane filter (0.1 µm pore size, Whatman™), which had preliminarily been washed with 4 mL 0.5 mg/mL Nd^{3+}-solution. The test tube was then rinsed with 2 mL 0.58 M HF and 2 mL H_2O dest. and the rinsing solutions were again filtered through the membrane filter, washing the precipitate as well. The filter was then dried and measured by alpha spectrometry.

4.2.2 Thorium-fraction

The Th-containing washing solution was evaporated to dryness and the resulting residue was evaporated three times with 5 mL HNO_3 conc. + 2 mL 30 w% H_2O_2, followed by triple evaporation with 5 mL HCl conc. The residue was dissolved in 2 mL 1 M HCl and the beaker was washed twice with 1 mL 1 M HCl. The combined solutions (4 mL total volume) were

transferred into a plastic test tube and co-precipitation with NdF_3 was performed as described in Chapter 4.2.1.

4.2.3 Plutonium-fraction

The Pu-containing washing solution was evaporated to dryness and the residue was evaporated three times with 5 mL HNO_3 conc. + 2 mL 30 w% H_2O_2, followed by triple evaporation with 5 mL HCl conc. The resulting residue was dissolved in 2 mL 1 M HCl and the beaker was washed two times with 1 mL 1 M HCl. The combined solutions (≙ 4 mL) were transferred into a plastic test tube and co-precipitation with NdF_3 was performed as described in Chapter 4.2.1.

4.2.4 Neptunium-fraction

The Np-fraction was evaporated to dryness and the residue was evaporated once with 5 mL HNO_3 conc. + 2 mL 30 w% H_2O_2. The resulting residue was dissolved in 20 mL 7.2 M HNO_3 and the solution was loaded on a TrisKem TEVA-column (Ø = 0.9 cm, filling level: 3.5 cm; conditioned with 7.2 M HNO_3). TEVA (also called Aliquat® 336; structure given in Figure 8) is mainly used to fix **TE**tra**VA**lent actinides and technetium.

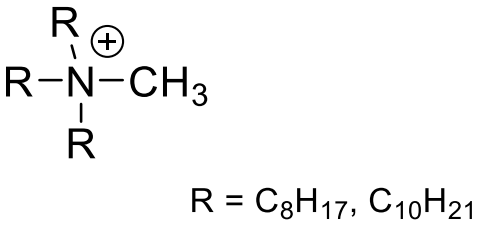

Figure 8: Structure of TEVA resin (Aliquat® 336)[49]

The beaker and the column were then washed with 5 mL 7.2 M HNO_3 respectively and the eluates from the loading as well as the washing solutions were discarded. Neptunium was eventually eluted with 20 mL 0.05 M HCl + 0.05 M HF. The solution was evaporated to dryness and the residue was evaporated three times with 5 mL HNO_3 conc. + 2 mL 30 w% H_2O_2, followed by triple evaporation with 5 mL HCl conc. The resulting residue was dissolved in 2 mL 1 M HCl and the beaker was rinsed twice with 1 mL 1 M HCl. The combined solutions (4 mL) were transferred into a plastic test tube and co-precipitation with NdF_3 was performed as described in Chapter 4.2.1.

4.2.5 Uranium

An overview of the sample treatment for analysis of uranium is shown in Figure 9.

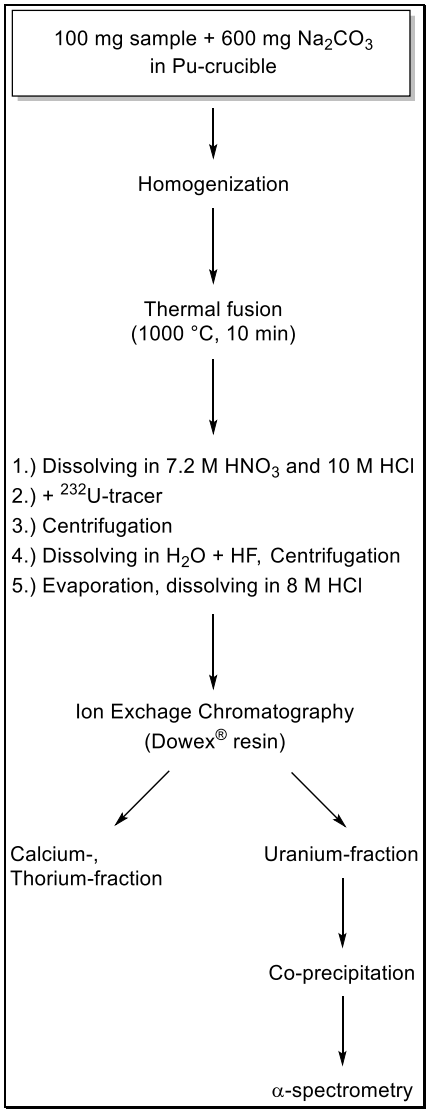

Figure 9: Schematic overview of sample treatment for alpha spectrometry of U (sample preparation to alpha spectrometry).

Sample preparation was conducted as described in Chapter 4.1. However, after centrifugation and evaporation of the solution, the residue was dissolved in 40 mL 8 M HCl and no oxidation state adjustment was performed as only U^{6+}-ions are present in the solution.

Separation of uranium was then conducted *via* anion exchange chromatography using a DOWEX® 1X2 (2 % cross-linkage) chloride form resin with a particle size of 100-200 mesh.[47] The chemical structure is shown in Figure 6. The prepared solution was loaded on the Dowex®-column (Ø = 1.3 cm, filling level: 6.5 cm; preliminarily conditioned with 8 M HCl), followed by rinsing of the beaker with 25 mL 8 M HCl and a further column washing step with 25 mL 8 M HCl. The eluates of the loading and washing solutions were combined and used for the

analysis of thorium (see also Chapter 4.2.2). Uranium was eventually eluted with 80 mL 0.1 M HCl. The U-solution was evaporated to dryness and the residue was evaporated three times with 5 mL HNO_3 conc. + 2 mL 30 w% H_2O_2, followed by triple evaporation with 5 mL HCl conc. The resulting residue was dissolved in 2 mL 1 M HCl, the beaker was rinsed twice with 1 mL 1 M HCl and combined solutions (4 mL) were transferred into a plastic test tube. 100 µL 0.5 mg/mL Nd^{3+}-solution and 7 - 10 drops of 15 w% $TiCl_3$-solution – reduces U^{6+} to U^{4+}, indicated by a pale purple solution – were added and uranium was co-precipitated with NdF_3 by the addition of 0.5 mL 40 w% HF. After waiting for 30 min, the solution was treated with ultrasound in a water bath for 1 min and was subsequently filtered through a cellulose nitrate membrane filter (0.1 µm pore size, Whatman™), which had preliminarily been washed with 4 mL 0.5 mg/mL Nd^{3+}-solution. The test tube was then rinsed with 2 mL 0.58 M HF and 2 mL H_2O dest. and the rinsing solutions were again filtered through the membrane filter, washing the precipitate as well. The filter was then dried and measured by alpha spectrometry.

4.2.6 Blanks

In order to determine the natural background concentrations and limits of detection of the analyzed actinides, blanks were prepared for each fraction as described in Chapter 4.2 and Chapters 4.2.1 to 4.2.5. No sample material and/or spikes were added, and fresh, non-contaminated glassware was used for this purpose.

4.2.7 Reference material

For the evaluation of the applied methods of chemical separation of the actinides a reference material – IAEA standard IAEA-375 ("Radionuclides in soil")[50] – was analyzed.

For this purpose, 10 - 20 g of reference material (~ 5 g for analysis of uranium) for each sample was weighed-in in a beaker and 150 mL 7.2 M HNO_3 were added. The suspension was then heated on a hot plate for ~2.5 h under reflux (leaching), followed by cooling to room temperature. After filtration of the dark-brown suspension and washing of the filter with 3 x 5 mL 8 M HNO_3, spikes were added (either ^{243}Am + ^{242}Pu, or ^{232}U; 10 µL each; activity concentrations are given in Table 5) and the filtrate was evaporated to dryness.

For the analysis of Am, Th and Pu, the residue was evaporated three times with 10 mL HNO_3 conc. + 5 mL 30 w% H_2O_2, followed by dissolving the resulting residue in 20 mL 1 M HNO_3.

100 mg Mohr's salt, 10 ml HNO_3 conc. and 0.5 g $NaNO_2$ were added in that order and the solution was then heated on a hot plate until formation of NO_x ceased. After cooling to room temperature, the red-orange solution was ready-to-use for ion exchange chromatography (see Chapter 4.2 and Chapters 4.2.1 to 4.2.3).

The residue from the solution for the analysis of U (contains ^{232}U-spike) was evaporated twice with 10 mL HNO_3 conc. + 5 mL 30 w% H_2O_2, followed by double evaporation with 10 mL HCl conc. each. The resulting residue was then dissolved in 40 mL 8 M HCl and the orange-yellow colored solution was ready-to-use for ion exchange chromatography (see Chapter 4.2.5).

4.2.8 AMS sample preparation

In order to confirm the presence of neptunium in the anion exchange chromatography fractions, the ^{237}Np/^{239}Pu-ratio was determined by accelerator mass spectrometry. For this purpose, the cellulose nitrate membrane filters of the neptunium fractions from the cryoconite samples (*Cryo. 3* and *Cryo. 9*) as well from the blanks were dissolved in 10 mL HNO_3 conc. Suprapur® in 50 mL Eppendorf tube and the solutions were then transferred into Teflon vials, followed by rinsing of the Eppendorf tube with 10 mL Milli-Q® H_2O each. 200 µL prenuclear Fe^{3+}-solution (1 mg/mL in ~3 M HCl) were added and the solutions were slowly evaporated at 60 °C. The resulting orange pellets (still containing filter residues) were then transferred with 3 x 1 mL HNO_3 conc. Suprapur® into microwave digestion vessels and microwave digestion was then performed in a Milestone Start 1500 microwave digestion system (start: 20 °C; 1. ramp: 43 °C min^{-1} linear to 150 °C; 2. ramp: 16 °C min^{-1} linear to 200 °C; 3. ramp: 3 °C min^{-1} linear to 230 °C; 10 min cooldown). After evolution of NO_x, the solutions were again transferred into Teflon vials and the microwave vessels were rinsed with Milli-Q® H_2O. The solutions were once again slowly evaporated at 60 °C over night and the resulting dark-orange residues were then transferred with 400 µL acetone into 1.5 mL Eppendorf vials, followed by rinsing of the Teflon vials with 200 µL acetone. After evaporation of the acetone for 2 hours at 40 °C, 1.8 mg PbF_2 were added to each vial (Fe/PbF_2 = 1/9). Sample preparation was stopped at this point because results from the latest actinide measurements indicated the need of an alteration in the AMS sample preparation procedure in order to minimize the loss of sample material during sample preparation. Further treatment of the samples, including AMS measurement, will be part of future experiments.

4.3 Analytical Methods

4.3.1 Alpha spectrometry

The activities of alpha emitters ^{241}Am, $^{239+240}$Pu, ^{238}Pu, ^{237}Np, ^{232}Th, ^{228}Th, ^{238}U, and ^{234}U were determined with a Canberra Model 7401VR alpha spectrometer with semiconductor detector (approximate counting efficiency of 30 %). The energy of the alpha particle is directly proportional to the amount of electron hole pairs created in the detector, hence allowing identification and quantification of the respective alpha source. Due to the short range of α-radiation and possible self-absorption, α-sources with as little matter as possible should be prepared. For this purpose, co-precipitation with NdF_3, followed by filtration through a membrane with small pore-size (0.1 µm Whatman™ Cellulose Nitrate Membrane Filter) was applied.[51] After filtration, a NdF_3 layer with approx. 10 µm thickness is formed. Measurement was then performed in an evacuated chamber. This method was selected because its advantages are the high sensitivity, due to its low background, and high selectivity, in respect of other types of radiation.[52]

4.3.2 Accelerator mass spectrometry

The ^{237}Np/^{239}Pu ratio in neptunium fractions was determined using accelerator mass spectrometry. Measurements were performed at the Institute of Isotope Physics, University of Vienna, with the Vienna Environmental Research Accelerator (VERA).

Generally, AMS is a highly sensitive method, allowing the accurate measurement of isotopic and atomic ratios.[53] Hereby, negative sample ions are created *via* cesium sputtering, which are subsequently mass-selected using electrostatic and magnetic fields. After injection into the accelerator, the ion charge is converted from negative to positive by knock-out of electrons with argon (p in µbar range) in a differentially pumped channel (the so-called 'stripper'). At this stage, all molecular ions are destroyed, and positive ions are accelerated a second time, resulting in an energy of several MeV. In the second mass spectrometer (analyzer), molecular break-up products are removed, and the target ions can be detected by an appropriate particle detector.[54] A schematic layout of the VERA facility at its current state is shown in Figure 10.

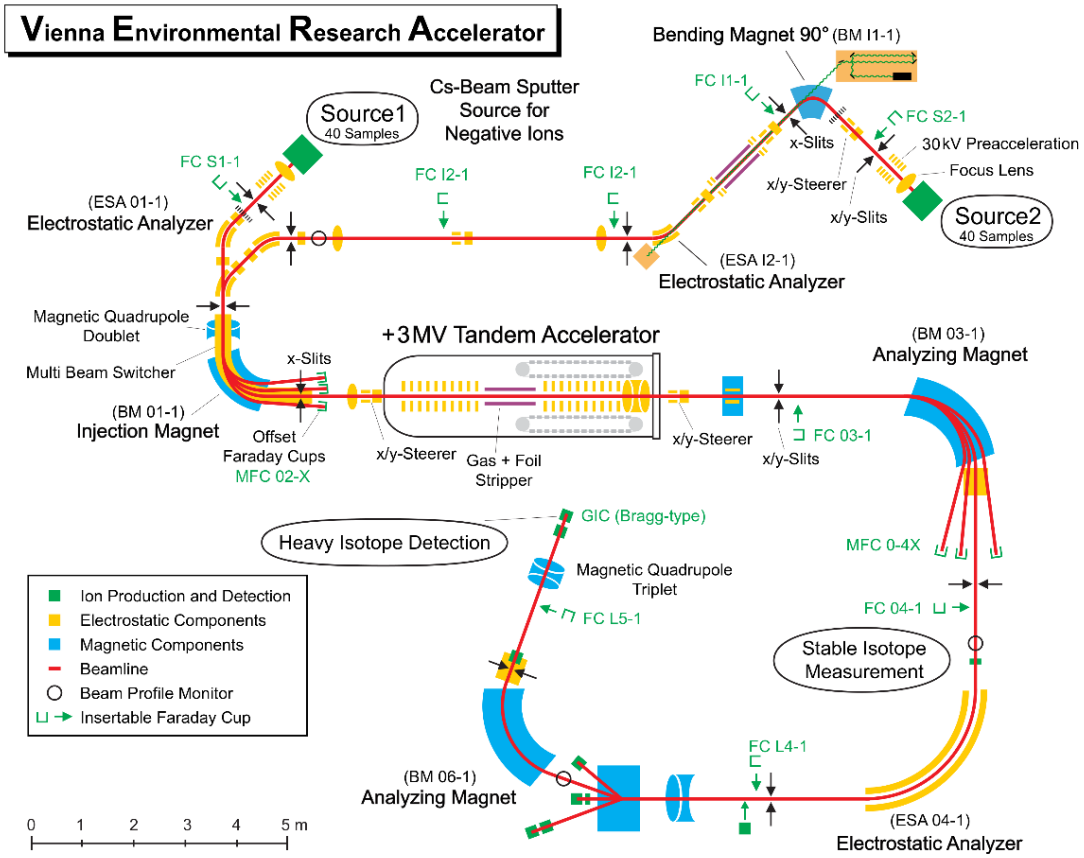

Figure 10: Current schematic layout of the VERA facility (modified version; original version from Ref [55]).

5 Results and Discussion

The overall results for the analyses of all four cryoconite samples by alpha spectrometry are given in Table 6. The results for each nuclide are discussed in separate sections. Spikes were used to quantify the true activity concentrations of the nuclides. A reference material (IAEA-375) was used to evaluate the chromatographic method, the results can be found in Section 5.6. In order to determine background radiation and to get an information about LOD values, blank samples were prepared and analyzed (for results see Section 5.7).

Table 6: Activity concentrations of the most important radionuclides determined in the cryoconite samples by alpha spectrometry. Values are stated in [Bq/kg dry matter] with experimental standard deviation (s; counting and sample preparation; 1σ error), decay corrected for October 2006. Note: n = number of samples used for calculation (in brackets).

Sample	$^{239+240}$Pu [Bq/kg]	s	^{238}Pu [Bq/kg]	s	^{241}Am [Bq/kg]	s	^{232}Th [Bq/kg]	s	^{238}U [Bq/kg]	s	^{234}U [Bq/kg]	s
Cryo. 1	3.3 (n = 1)	0.6	1.59 (1)	0.45	4.1 (1)	0.7	42.7 (1)	7.4				
Cryo. 3	134.4 (3)	4.1	10.24 (3)	0.75	65.3 (1)	1.8	36.8 (1)	4.4				
Cryo. 7	12.5 (3)	1.2	3.36 (3)	0.61	7.6 (1)	0.8	34.9 (2)	4.4	38.2 (1)	1.7	35.5 (1)	1.6
Cryo. 9	121.8 (3)	5.1	6.22 (4)	0.84	57.6 (1)	3.1	35.8 (1)	6.4				

5.1 Plutonium results

In general, plutonium data corresponds with previously reported data.[42,43] However, ^{238}Pu values are higher for all measured samples. The major difference in sample preparation was the use of thermal fusion as chemical pulping, in comparison to repeated evaporation with acid used by Tieber *et al.*[42] and M. Bartmann.[43] $^{239+240}$Pu values considerably better match the reported data, suggesting that thermal fusion is a comparable process for cryoconite sample digestion besides leaching. Figures 11-15 show the comparison of the previously reported values for the cryoconite samples *(Cryo. 1, Cryo. 3, Cryo. 7, Cryo. 9*) with the values obtained in this study.

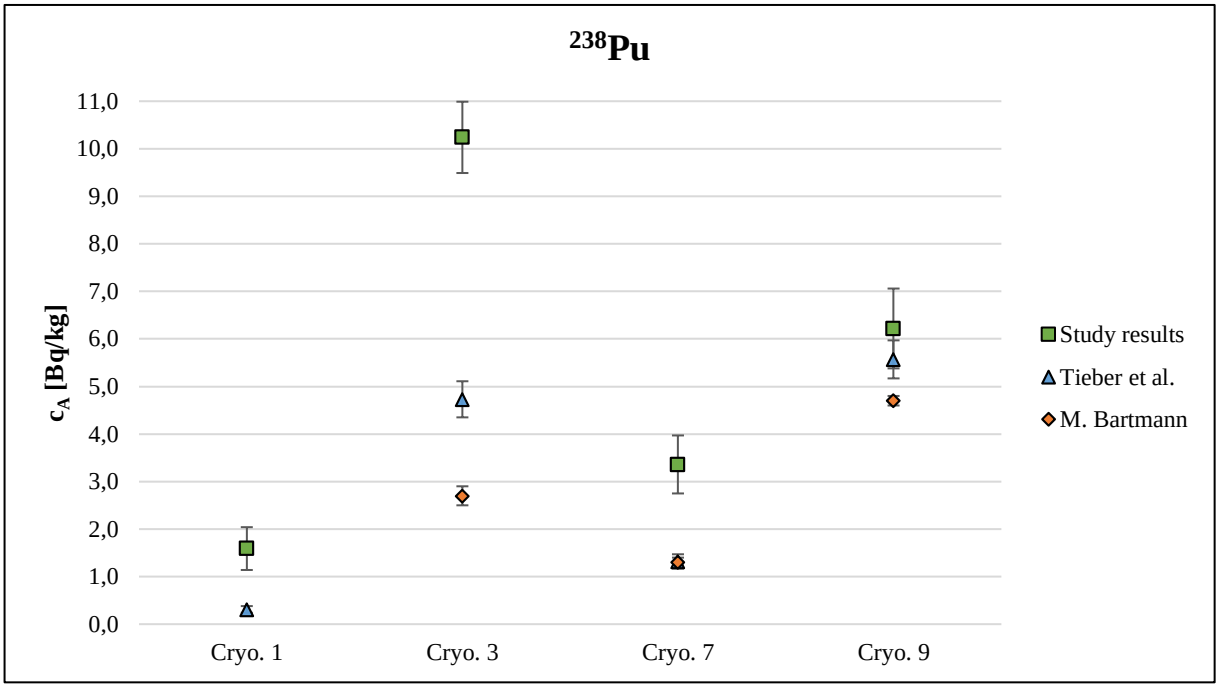

Figure 11: Comparison of previously reported ^{238}Pu activity concentrations data obtained in this study. Activity concentration (c_A) is stated in [Bq/kg dry matter] with experimental standard deviation error bars.

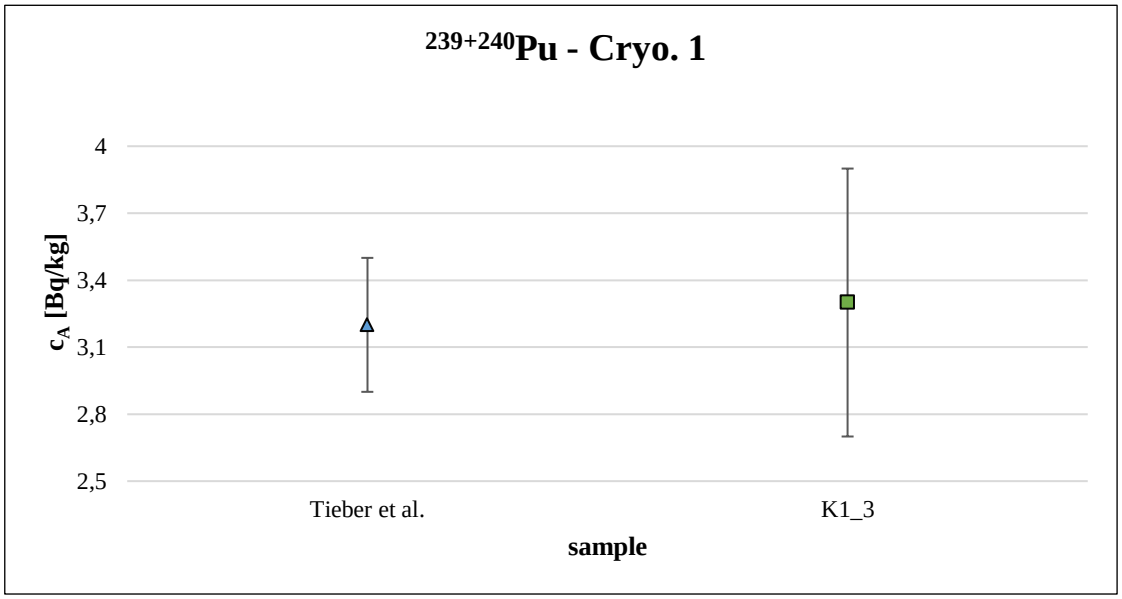

Figure 12: Comparison of previously reported $^{239+240}$Pu activity concentration by Tieber *et al.* (triangle) in cryoconite sample *Cryo. 1* with data obtained in this study (square). Activity concentration (c_A) is stated in [Bq/kg dry matter] with experimental standard deviation error bars.

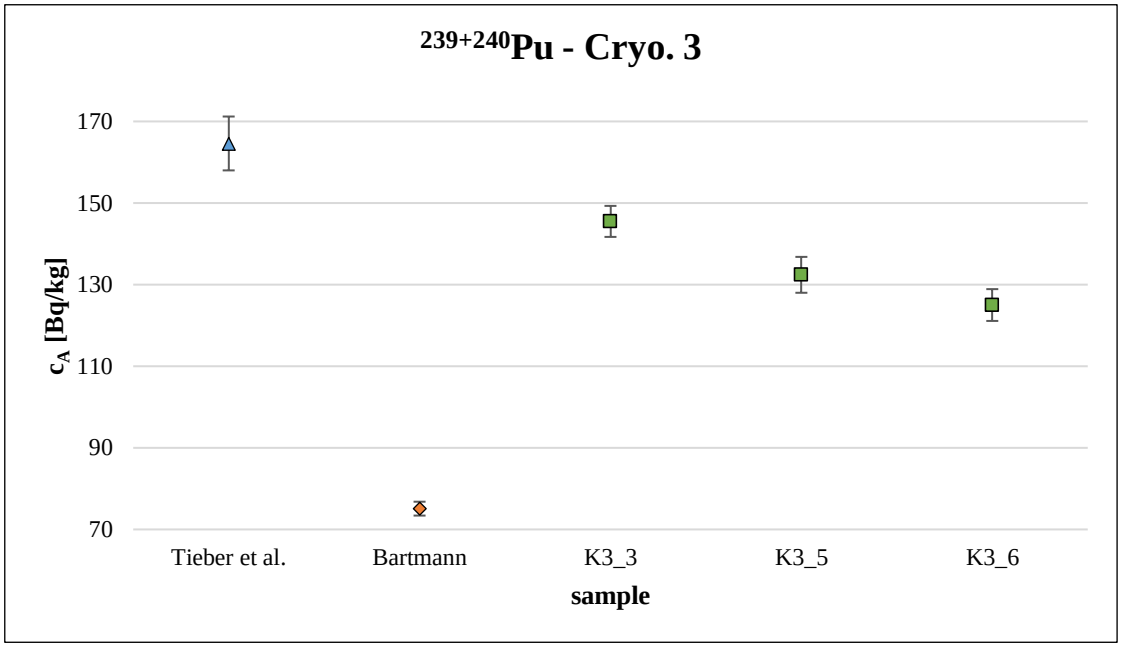

Figure 13: Comparison of previously reported $^{239+240}$Pu activity concentrations by Tieber *et al.* (triangle) and M. Bartmann (rhomb) in cryoconite sample *Cryo. 3* with data obtained in this study (square). Activity concentration (c_A) is stated in [Bq/kg dry matter] with experimental standard deviation error bars.

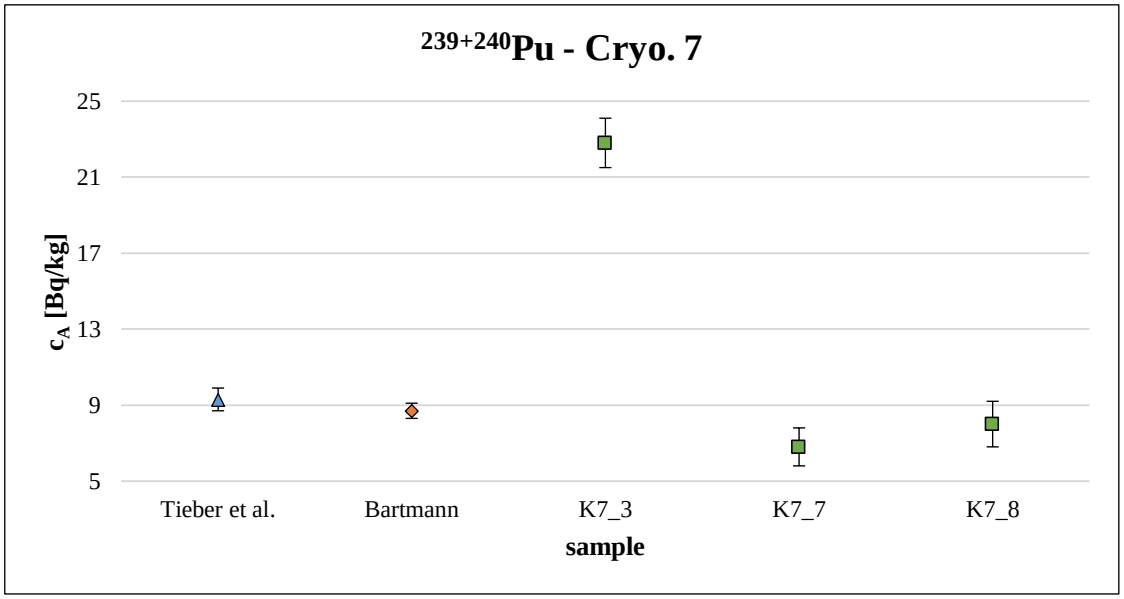

Figure 14: Comparison of previously reported $^{239+240}$Pu activity concentrations by Tieber *et al.* (triangle) and M. Bartmann (rhomb) in cryoconite sample *Cryo. 7* with data obtained in this study (square). Activity concentration (c_A) is stated in [Bq/kg dry matter] with experimental standard deviation error bars.

Although one might assume that the $^{239+240}$Pu activity concentration value for sample *K7_3* is an outlier (see Figure 14), a Grubbs's test revealed that it is indeed furthest from the rest, but not a significant outlier ($P > 0.05$). It was therefore used for the calculation of the mean value.

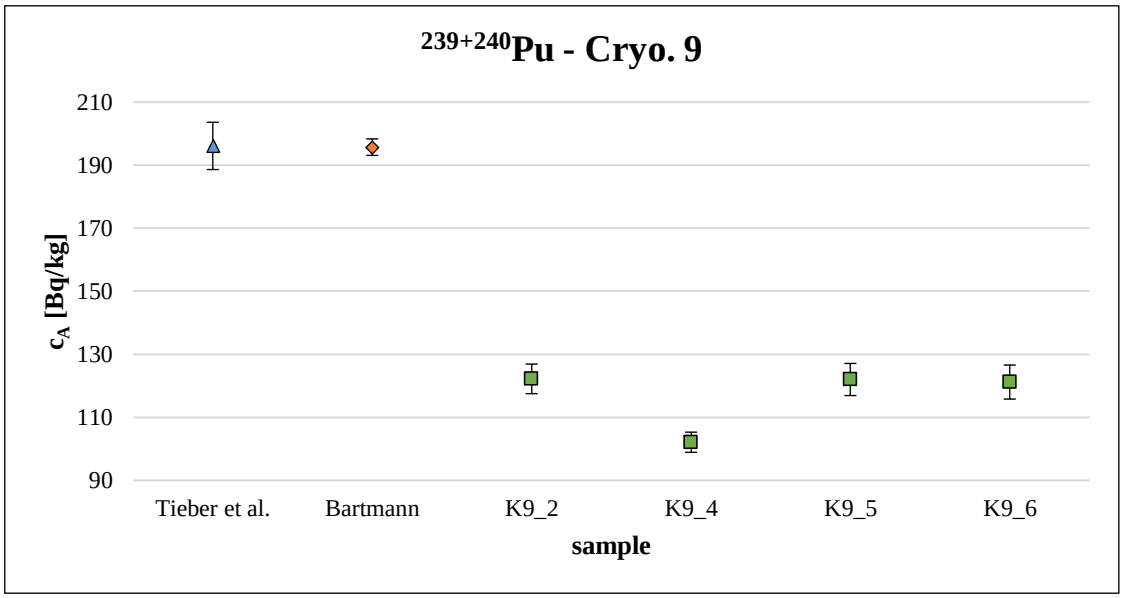

Figure 15: Comparison of previously reported $^{239+240}$Pu activity concentrations by Tieber *et al*. (triangle) and M. Bartmann (rhomb) in cryoconite sample *Cryo. 9* with data obtained in this study (square). Activity concentration (c_A) is stated in [Bq/kg dry matter] with experimental standard deviation error bars.

While in Figure 14 sample *K7_3* seemed to be an obvious outlier (the hypothesis could not be confirmed), sample *K9_4* (see Figure 15) is indeed a significant outlier (Grubbs's test; $P < 0.05$) and the value was excluded from the mean value calculation.

Above figures only show the results for the 'newly tested' fusion method, where the spike was added after thermal fusion at 1000 °C. Some experiments were performed using either leaching or fusion method with spikes added before digestion. Here the results deviate from the mean values stated in Table 6 (stated "standard" fusion method). These results are depicted in Figure 16.

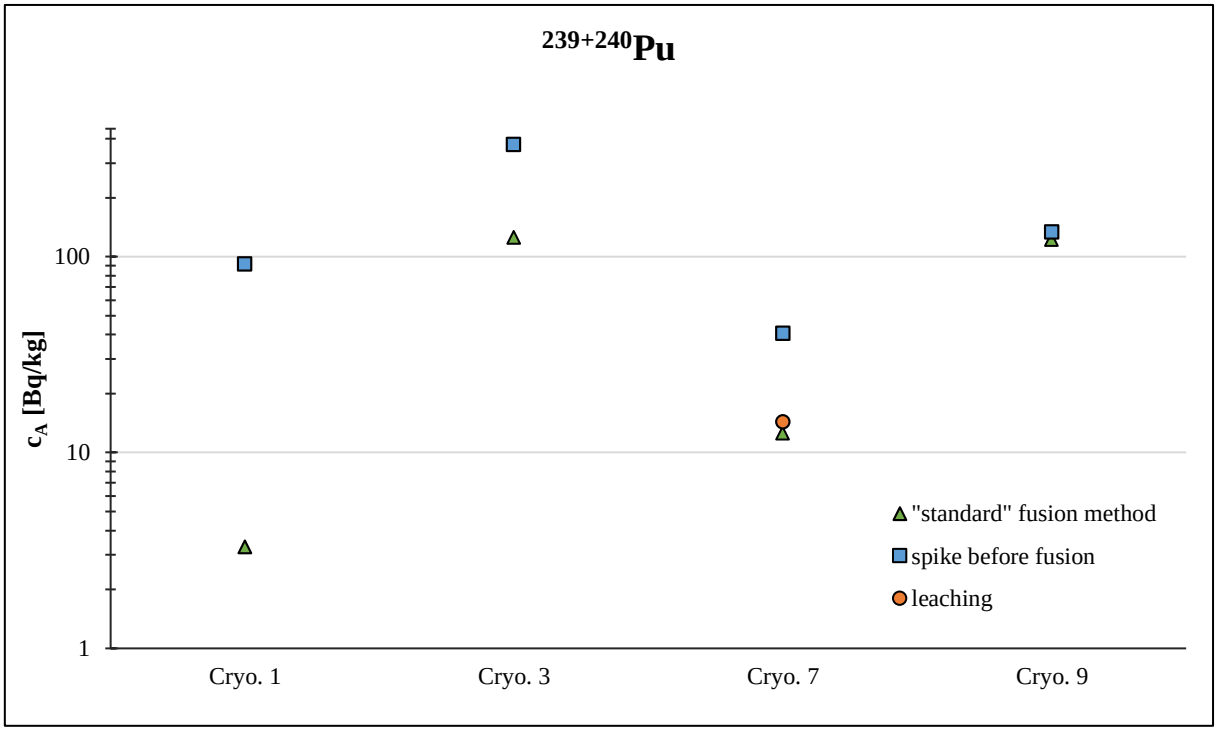

Figure 16: Comparison of $^{239+240}$Pu activity concentrations in cryoconite samples deriving from different sample preparation methods. Activity concentration (c_A) is stated in [Bq/kg dry matter].

Using the leaching method during sample preparation does not seem to diverge from the fusion method results. However, it was only tested for one sample, hence the data is inconclusive and further experiments might be carried out to directly compare both methods.

Adding the ^{242}Pu-spike before thermal fusion seems to result in a significant increase in plutonium activity concentration (all samples except *Cryo. 9*). This phenomenon might be explained by a loss of spike in the furnace, thus altering the 'true' ^{242}Pu/$^{239+240}$Pu ratio in the sample solution after ion exchange chromatography. In theory it should be impossible because the mixture of cryoconite sample and spike solution had been dried before adding Na_2CO_3 and placing it in the furnace. Since plutonium is known for its complex chemistry (see also Chapter 2.3.1) anyway, further studies on the influence of the moment of spike addition on the activity concentration results might be carried out in the future.

5.2 Americium results

Americium activity concentration was measured in all four cryoconite samples. The results are given in Table 6. Figure 17 shows the comparison of the result with the previously reported values by Tieber *et al.*[42]

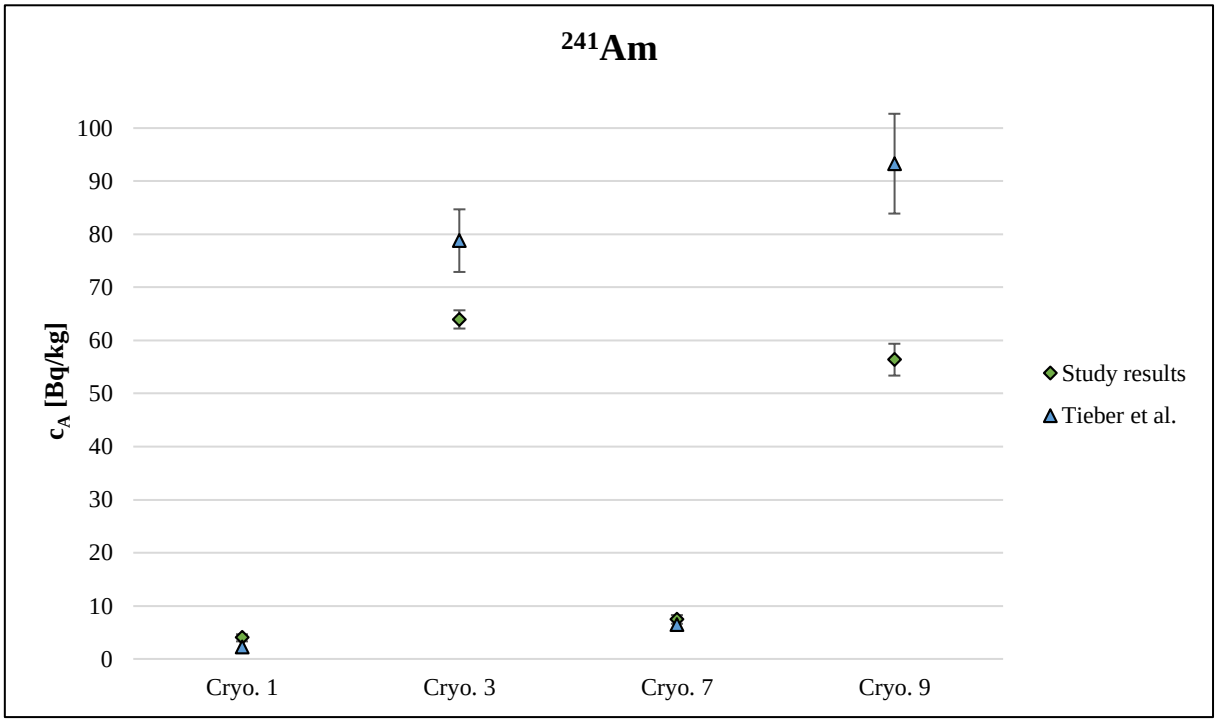

Figure 17: Comparison of previously reported ^{241}Am activity concentrations by Tieber *et al.* (triangle) with data obtained in this study (rhomb). Activity concentration (c_A) is stated in [Bq/kg dry matter] with experimental standard deviation error bars.

^{241}Am values are of the same order of magnitude as the $^{239+240}$Pu values, which is normally found in environmental samples. The values reported by Tieber and co-workers are of the same order of magnitude, too. However, the values of the older population (*Cryo. 3* and *Cryo. 9*; see also Figure 3) are lower than the reported values, whereas the values of the younger population (*Cryo. 1* and *Cryo. 7*) are a little higher and above detection limit. In general, the values obtained in this study match the ones reported by Tieber *et al.*, with more americium being found in the samples dominated by Chernobyl fallout (younger population). Other studies (e.g. Owens *et al.*[4]) also confirm this conclusion.

Since no strong deviation from the previously reported values could be observed, thermal fusion combined with the described ion exchange separation method might be used as a standard sample preparation method in the future. However, this assumption still depends on further studies, hopefully to be carried out.

5.2.1 Original ^{241}Pu activity concentration and ^{241}Pu/$^{239+240}$Pu activity ratio

Activity concentrations of the nuclide ^{241}Pu can be determined directly from the values of daughter nuclide ^{241}Am. Their activity concentrations are related according to Eq. **(24)**.

$$A_{^{241}Pu}(t=0) = A_{^{241}Am}(t) * \frac{\lambda_{Pu}-\lambda_{Am}}{\lambda_{Am}(e^{-\lambda_{Am}*t}-e^{\lambda_{Pu}*t})} \quad \textbf{(24)}$$

One can assume that most of the plutonium was released into the environment during nuclear weapon testing in the middle of the 20th century, with the so-called 'bomb peak' in 1963. With t = 57 a (1963 to 2020) and the respective decay constants (^{241}Pu: 0.0484 a^{-1} and ^{241}Am: 0.0016 a^{-1}) Eq. **(24)** reduces to

$$A_{^{241}Pu}(0) = A_{^{241}Am} * 34.37 \quad \textbf{(25)}$$

The calculated ^{241}Pu activity concentrations and ^{241}Pu/$^{239+240}$Pu activity ratios (using the values stated in Table 6) for all cryoconite samples for the year 1963 are given in Table 7.

Table 7: ^{241}Pu activity concentrations (stated in [Bq/kg]) and ^{241}Pu/$^{239+240}$Pu ratios for all analyzed cryoconite samples.

Sample	^{241}Pu [Bq/kg]	s	^{241}Pu/$^{239+240}$Pu	s
Cryo. 1	137	23	41.3	10.4
Cryo. 3	2198	59	16.4	0.7
Cryo. 7	12.5	28	20.4	2.9
Cryo. 9	1938	103	15.9	0.9

Analogous to the ^{241}Am activity concentrations, the ^{241}Pu/$^{239+240}$Pu activity ratios divide into two groups. The values for *Cryo. 3* and *Cryo. 9* (16.4 and 15.9, respectively) perfectly match data reported for nuclear weapon test fallout (^{241}Pu/$^{239+240}$Pu = 16)[56], therefore supporting the conclusion of Tieber *et al.*, with these cryoconite samples belonging to the 'older' group, which is mainly dominated by nuclear weapon fallout (see also Chapter 2.4.1). By contrast, *Cryo. 1* and *Cryo. 7* belong to the group dominated by Chernobyl fallout. This is also reflected in their elevated ^{241}Pu/$^{239+240}$Pu activity ratios (41.3 and 20.4, respectively), indicating a possible contribution of ^{241}Pu deriving from Chernobyl fallout (^{241}Pu/$^{239+240}$Pu = 86).[56]

5.3 Thorium results

Thorium activity concentrations were calculated by the evaluation of the overall average chemical yield. ^{232}U-spike – in radioactive equilibrium with ^{228}Th – was added to some sample solutions of *Cryo. 7* after thermal fusion, increasing the ^{228}Th counts in the alpha spectrum. An average ^{228}Th/^{232}Th ratio was calculated from the samples without spike. In the spiked sample, ^{232}Th counts were then multiplied with the average ^{228}Th/^{232}Th ratio, giving the actual ^{228}Th-counts of the cryoconite sample. Subtraction from the total, measured ^{228}Th-counts then gave the counts deriving from the spike, thus allowing the calculation of the chemical yield.

The activity concentrations for all cryoconite sample (35.8 ± 6.4 to 42.7 ± 7.4 Bq/kg; see also Table 6) are in good correspondence with values reported in literature[57] (25 – 50 Bq/kg worldwide mean value in soil), thus seeming plausible.

5.4 Uranium results

One cryoconite sample (*Cryo. 7*) was analyzed for its uranium content. The results are given in Table 8, compared to the reported values of the same sample from M. Bartmann.[43]

Table 8: Activity concentrations of uranium isotopes determined in the cryoconite sample *Cryo. 7* by alpha spectrometry, compared to previously reported values. Values are stated in [Bq/kg dry matter] with experimental standard deviation (s; counting and sample preparation; 1σ error), decay corrected for October 2006.

Sample	^{238}U [Bq/kg]	s	^{234}U [Bq/kg]	s
Cryo. 7	38.2	1.7	35.5	1.6
M. Bartmann[43]	17.0	1.1	18.5	1.1

The alpha spectrometry results for uranium are not very conclusive, since only one sample was analyzed. But the activity concentration values are approximately twice as high as the ones reported by M. Bartmann. This might be due to a smaller loss of uranium during sample preparation, when thermal fusion is applied. However, further experiments need to be carried out to verify this assumption.

5.5 Neptunium results

Results for the neptunium determination are not stated in this thesis because measurements by AMS could not be performed to date. Alpha spectrometry provides data, which can only be used to estimate the ^{237}Np/$^{239+240}$Pu ratio in the samples. This is due to an overlay of peaks from

different possible nuclides in the spectrum area around 4.788 MeV, neptunium's alpha energy with the highest intensity. But it is estimated, that in a best-case scenario the ratio varies between 38.7 and 177.9, which would be far higher than previously reported values[58], thus indicating a good separation of neptunium from plutonium during ion exchange chromatography.

5.6 Reference material results

As mentioned in Section 4.2.7, a reference material was analyzed to evaluate the applied methods of chemical separation of the actinides. IAEA standard IAEA-375 ("Radionuclides in soil") was chosen for this purpose. The fusion method itself could not be evaluated because the nuclides were separated from the reference material *via* leaching in hot acid, which is an easier method for larger amounts of sample material. The results for the reference material (two reference samples were analyzed independently) are given in Table 9.

Table 9: Measured and referenced activity concentrations – including 95 % confidence interval – of nuclides in reference material IAEA-375. Values are stated in [Bq/kg dry matter] with experimental standard deviation (s; counting and sample preparation; 1σ error), decay corrected for December 1991.

Analyte	Sample 1 [Bq/kg]	s	Sample 2 [Bq/kg]	s	Mean Value [Bq/kg]	s	Reference value[50] [Bq/kg]	95 % C.I.[50]
^{241}Am	0.33	0.01	0.57	0.03	0.45	0.02	0.13	0.11 – 0.15
$^{239+240}$Pu	0.35	0.02	0.36	0.02	0.36	0.02	0.30	0.26 – 0.34
^{238}Pu	0.095	0.008	0.100	0.012	0.097	0.010	0.071	0.056 – 0.085
^{232}Th	10.8	1.9	11.9	1.3	11.3	1.6	20.5	19.2 – 21.9
^{228}Th	11.1	1.9	12.2	1.3	11.6	1.6	21	17 – 25
^{238}U	14.3	0.3	13.6	0.7	13.9	0.6	24.4	19.0 – 29.8
^{234}U	14.8	0.3	13.9	0.7	14.4	0.6	25	17 – 32

The results for the reference material show 'two groups' of nuclides. Measured americium and plutonium values are higher than the reference values. However, plutonium values match the ones stated in the reference sheet quite well; therefore, it can be assumed that the method for the separation of plutonium is suitable. The measured americium value exceeds the reference value by a factor of three but stays within the same order of magnitude. The number of accepted laboratories, that were participating in the calculation of the ^{241}Am activity concentration value is significantly lower than for the calculation of the plutonium value. If more laboratories had been taking part, the mean value might have been higher. Furthermore, it needs to be considered

that the reference values are stated as 'information values', hence their significance needs to be scrutinized. Nonetheless they are still important indicators for the evaluation of the applied analytical method.

The second 'nuclide group' consists of the thorium and uranium isotopes. The measured values are significantly lower than the 'information values' (^{228Th}, ^{234}U, ^{238}U) and the 'recommended value' (^{232}Th), and even far outside the 95 % confidence interval. One possible reason for this phenomenon might be the larger amounts of reference material that were used in sample preparation, since the activity concentrations of americium and plutonium were expected to be low. Thorium concentrations in the reference material and in the sample material (cryoconites) are approximately of same order of magnitude, but with a 100 to 200-fold amount of total thorium (~ 10 to 20 g reference material vs. ~ 0.1 g cryoconite sample material) the capacity of the ion exchange column might be exceeded. However, this might only be the case for thorium because the uranium samples were prepared separately (see also Section 4.2.7). In the case of thorium, it is also important to keep in mind that the chemical yield was calculated indirectly in a separate experiment (with a ^{232}U-spike) because no non-interfering thorium-spike had been available. Therefore, the stated values are merely assumptions.

5.7 Blank results

Background activity values for all measured nuclides were calculated measuring blank samples. For this purpose, fresh glassware was used for each experiment. The results are summarized in Table 10.

Table 10: Mean background activities of all radionuclides of importance. Values are stated in [mBq] with experimental standard deviation (s; counting and sample preparation; 1σ error; n = 2)

Analyte	Measurement time [s]	Mean background [mBq]	s
^{241}Am	431785	0.07	0.03
^{243}Am	431785	0.10	0.03
$^{239+240}$Pu	600000	0.27	0.05
^{238}Pu	600000	0.25	0.05
^{242}Pu	600000	0.15	0.04
^{232}Th	600000	0.21	0.04
^{228}Th	600000	0.20	0.04
^{238}U	346000	0.04	0.02
^{234}U	346000	0.07	0.03
^{232}U	346000	0.13	0.04

All mean blank values are in a sufficiently low order of magnitude and no signs of heavy contamination seem to exist. Neptunium blanks could not be analyzed by alpha spectrometry because the exact position of the ^{237}Np peak in the spectrum was unclear, but future AMS measurements might provide information about the neptunium background. The uranium blanks will also be part of future AMS measurements because previous studies[43] indicated a contamination from an unknown source, visible through an increased ^{236}U/^{238}U ratio.

In order to determine if all results are above the detection limit, blank results were also used for the calculation of the LOD for each sample (see Eq. **(26)**).[59] For abbreviations see Section 8.

$$LOD = \left(2.71 + 4.65 * \sqrt{cps_{blank} * t_{meas_{sample}}}\right) * \frac{A_{spike}}{cts_{spike}} \quad \textbf{(26)}$$

A_{spike} is the activity in [mBq] of the spike added to the cryoconite sample, cts_{spike} is the number of total counts of the added spike in the cryoconite sample, cps_{blank} are the counts per second of the respective desired nuclide in the blank sample, and $t_{meas,sample}$ is the measurement time in [s] of the cryoconite sample.

LOD-values for a typical sample prepared with standard fusion method are given in Table 11.

Table 11: Typical limits of detection for different radionuclides in cryoconite samples (calculated using Eq. 24). Values are stated in [mBq].

Analyte	$t_{meas,sample}$ [s]	A_{spike} [mBq]	cts_{spike}	cps_{blank} [s^{-1}]	LOD [mBq]
^{241}Am	500000	46.3	6412	$2.55 \cdot 10^{-5}$	0.14
$^{239+240}Pu$	800000	14.4	2669	$9.33 \cdot 10^{-5}$	0.23
^{238}Pu	800000	14.4	2669	$1.83 \cdot 10^{-5}$	0.11
^{234}U	590000	17.0	2884	$2.46 \cdot 10^{-5}$	0.12
^{238}U	590000	17.0	2884	$1.06 \cdot 10^{-5}$	0.08

6 Summary and Outlook

6.1 Summary

Cryoconite samples (*Cryo. 1, Cryo. 3, Cryo. 7, Cryo. 9)*, collected by Tieber and co-workers (University of Salzburg) at the Hallstätter and Schladminger glacier (Upper Austria) in 2006, were analyzed to determine their actinide content, primarily $^{239+240}$Pu and ^{241}Am. Activity concentrations were expected to be high, as cryoconites are sources for almost pure fallout values due to the lack of dilution with other organic/inorganic matter.

Alpha spectrometry was used to measure the radionuclide content in the NdF_3-layer after sample preparation. Different from previous studies[42,43], thermal fusion with sodium carbonate, followed by dissolving in inorganic acids (HNO_3, HCl, HF) was used to obtain a sample solution for the ion exchange chromatography. In this study, additional separation steps were necessary to obtain individual americium and neptunium fractions. To evaluate the sample preparation and separation methods, a reference material (IAEA-375) was analyzed, too.

In general, the results correspond well with the previously reported data, with ^{241}Am and $^{239+240}$Pu activity concentrations of 4.1 to 65.3 Bq/kg and 3.3 to 134.4 Bq/kg, respectively. However, the values of the so-called 'old population' (see also Chapter 2.4.1) are significantly lower than the ones reported by Tieber *et al.* and M. Bartmann – e.g. 121.8 Bq/kg versus 196.1 and 195.7 Bq/kg, respectively. ^{238}Pu activity concentrations exceed the reported values by up to a factor of 2, but generally are of the same order of magnitude. With the use of the ^{241}Am activity concentrations, the original concentrations (for the year 1963) of the short-lived mother nuclide ^{241}Pu and the ^{241}Pu/$^{239+240}$Pu activity ratios were calculated. The results strengthened the findings of Tieber *et al.*, who stated the existence of two different cryoconite groups, influenced by either nuclear weapon or Chernobyl fallout.

^{232}Th activity concentrations in the cryoconite samples were measured using a ^{232}U-spike (in radioactive equilibrium with ^{228}Th). With activity concentrations between approximately 36 and 43 Bq/kg, the results are in good correspondence with the worldwide mean values for soil reported in literature (25 to 50 Bq/kg).

Uranium activity concentrations were measured as well, although only in one sample (*Cryo. 7*). For this sample, M. Bartmann reported values of 17.0 and 18.5 Bq/kg for ^{238}U and ^{243}U, respectively, while in this study activity concentrations of 38.2 and 35.5 Bq/kg could be

obtained. However, the influence of the difference in sample preparation on the results needs further investigation.

In addition, AMS samples of the neptunium fractions were prepared in order to quantify ^{237}Np in Austrian samples for the first time.

In conclusion, the new sample preparation and ion exchange separation procedure was successfully used to reproduce previous activity concentration results for the cryoconite samples and evaluation with a reference material also seemed to confirm its potential. One advantage of thermal fusion in sample preparation might be the reduced sample material consumption. This fact could make it the method of choice for future experiments, in which homogenous samples (like cryoconites) with a high concentration of radionuclides are analyzed and sample material is scarce.

6.2 Outlook

First and foremost, the suitability of the applied sample preparation methods (thermal fusion and ion exchange chromatography procedure) needs to be reviewed by rerunning the experiments with the same cryoconite samples. One might also focus a little more on the analysis of thorium and uranium. Regarding thorium, a spike that can be measured independently from ^{232}Th and ^{228}Th, thus making double sample preparation obsolete, might be of interest.

Another important future task is the analysis of ^{237}Np in the cryoconite samples. Separate neptunium fractions could be obtained in this study, but analysis of the samples and blanks with accelerator mass spectrometry remains pending. If the results are positive, neptunium analysis can be extended to more samples (cryoconites and other). This would provide a long-awaited insight into the topic of neptunium in Austrian samples.

7 References

[1] Kónya, J.; Nagy, N. M., *Nuclear and Radiochemistry*, 1st ed. Elsevier, London, **2012**.

[2] Lettner, H.; Griesebner, A.; Peer, T.; Hubmer, A. K.; Pintaric, M., *J. Environmental Radioactivity*, **2006**, *86*, 12-30.

[3] Wilflinger, T.; Lettner, H.; Hubmer, A.; Bossew, P.; Sattler, B.; Slupetzky, H., *J. Environmental Radioactivity*, **2018**, *186*, 90-100.

[4] Owens, P. N.; Blake, W. H.; Millward, G. E., *Scientific Reports*, **2019**, *9*, 1-9.

[5] Blais, J. M.; Schindler, D. W.; Muir, D. C. G.; Kimpe, L. E.; Donald, D. B.; Rosenberg, B., *Nature*, **1998**, *395*, 585-588.

[6] Ferrario, C.; Finizio, A.; Villa, S., *Sci. Total Environ.*, **2017**, *574*, 350-357.

[7] Blais, J. M.; Schindler, D. W.; Muir, D. C.; Sharp, M. T.; Donald, D. K.; Lafreniere, M.; Braekevelt, E.; Strachan, W.M., *Ambio*, **2001**, *30*, 410-415.

[8] Rutherford, E., *Philosophical Magazine*, **1899**, *47*, 109-163.

[9] Rutherford, E.; Royds, T., *Philosophical Magazine*, **1908**, *16*, 313-317.

[10] Wernick, M. N.; Aarsvold, J. N., *Emission Tomography: The Fundamentals of PET and SPECT*, 1st ed. Elsevier Academic Press, Amsterdam, **2004**.

[11] Alvarez, L. W., *Physical Review*, **1937**, *52*, 134-135.

[12] Rutherford, E., *Philosophical Magazine*, **1903**, *5*, 177-187.

[13] Legrand, J.; Clement, C., *Int. J. Appl. Radiation Isotopes*, **1972**, *23*, 225-227.

[14] Curie, I.; Joliot, F., *Journal de Physique et le Radium*, **1933**, *4*, 278-286.

[15] Jackson, K. P.; Cardinal, C. U.; Evans, H. C.; Jelley, N. A.; Cerny, J., *Phys. Lett. B*, **1970**, *33*, 281-283.

[16] Scharff-Goldhaber, G.; Klaiber, G. S., *Physical Review*, **1946**, *70*, 229.

[17] Rose, H. J.; Jones, G. A., *Nature*, **1984**, *307*, 245-247.

[18] Asti, M.; De Pietri, G.; Fraternali, A.; Grassi, E.; Sghedoni, R.; Fioroni, F.; Roesch, F.; Versari, A; Salvo, D., *Nucl. Med. Bio.*, **2008**, *35*, 721-724.

[19] Seaborg, G. T.; McMillan, E. M.; Kennedy, J. W.; Wahl, A. C., *Physical Review*, **1946**, *69*, 366-367.

[20] Seaborg, G. T.; Wahl, A. C.; Kennedy, J. W., *Physical Review*, **1946**, *69*, 367.

[21] Vajda, N.; Kim, C.-K., *J. Radioanal. Nucl. Chem.*, **2010**, *283*, 203-223.

[22] National Center for Biotechnology Information. PubChem Database. Plutonium, CID=23940, <https://pubchem.ncbi.nlm.nih.gov/compound/Plutonium> (retrieved May 6, 2020)

[23] Live Chart of Nuclides, IAEA Nuclear Data Section, **2020**,

<https://www-nds.iaea.org/relnsd/vcharthtml/VChartHTML.html>

(retrieved May 6, 2020)

[24] Harley, J. H., *J. Radiation Research*, **1980**, *21*, 83-104.

[25] Salminen-Paatero, S.; Nygren, U.; Paatero, J., *J. Environ. Rad.*, **2012**, *113*, 163-170.

[26] Kelley, J. M.; Bond, L. A.; Beasley, T. M., *Sci. Total Environ.*, **1999**, *237/238*, 483-500.

[27] Seaborg, G. T., *Science*, **1946**, *104*, 379-386.

[28] Pepling, R. S., *Chemical & Engineering News*, **2003**, *81*, 170.

[29] McMillan, E.; Abelson, P. H., *Physical Review*, **1940**, *57*, 1185-1186.

[30] English, A. C.; Cranshaw, T. E.; Demers, P.; Harvey, J. A.; Hincks, E. P.; Jelley, J. V.; May, A. N., *Physical Review*, **1947**, *72*, 253-254.

[31] Giroux, R., *Chemical & Engineering News*, **2003**, *81*, 168.

[32] Weeks, M. E., *J. Chem. Education*, **1932**, *9*, 1231-1243.

[33] Ade, P. A. R.; Aghanim, N.; Arnaud, M.; Ashdown, M.; Aumont, J.; Baccigalupi, C.; Banday, A. J.; Barreiro, R. B.; Bartlett, J. G.; Bartolo, N.; *et al*, *Astronomy & Astrophysics*, **2016**, *594*, A13/1-A13/6.

[34] Grae, S. H., *Chemical & Engineering News*, **2003**, *81*, 163.

[35] Eichstaedt, P., *Chemical & Engineering News*, **2003**, *81*, 165.

[36] Łokas, E.; Zaborska, A.; Kolicka, M.; Rozycki, M.; Zawierucha, K., *Chemosphere*, **2016**, *160*, 162-172.

[37] Podgorny, I. A.; Grenfell, T. C., *Geophys. Res. Lett.*, **1996**, *23*, 2465-2468.

[38] Takeuchi, N.; Nishiyama, H.; Li, Z., *Ann. Glaciol.*, **2010**, 9-14.

[39] Takeuchi, N., *Ann. Glaciol.*, **2002**, *34*, 409-414.

[40] Kumada, K., *Soil Sci. Plant Nutr.*, **1965**, *11*, 11-16.

[41] Łokas, E.; Zaborska, A.; Kolicka, M.; Rozycki, M.; Zawierucha, K., *Chemosphere*, **2016**, *160*, 162-172.

[42] Tieber, A.; Lettner, H.; Bossew, P.; Hubmer, A.; Sattler, B.; Hofmann, W., *J. Environmental Radioactivity*, **2009**, *100*, 590-598.

[43] Bartmann, M., *Analysis of Actinides in Cryoconites (MSc Thesis)*, University of Vienna,Vienna, **2019**.

[44] Becker, J. S.; Dietze, H.-J., *Fresenius' Journal of Analytical Chemistry*, **1999**, *365*, 429-434.

[45] Mietelski, J. W.; Kierepko, R.; Łokas, E.; Cwanek, A.; Kleszcz, K.; Tomankiewicz, E.; Mroz, T.; Anczkiewicz, R.; Szalkowski, M.; Was, B.; Bartyzel, M.; Misiak, R., *J. Radioanal. Nucl. Chem.*, **2016**, *310*, 661-670.

[46] Dowex® 1x8, Product catalogue, Sigma-Aldrich,

<https://www.sigmaaldrich.com/catalog/product/sial/217425?lang=de&region=AT> (retrieved May 6, 2020)

[47] Dowex® 1x2, Product catalogue, Sigma-Aldrich,

<http://www.sigmaaldrich.com/catalog/product/sial/217387?lang=de&region=AT> (retrieved May 6, 2020)

[48] TRU resin Product Sheet, TrisKem International,

<https://www.triskem-international.com/scripts/files/5c5864afe022b8.73251229/PS_TRU-Resin_EN_161007.pdf>

(retrieved May 6, 2020)

[49] TEVA resin Product Sheet, TrisKem International,

<https://www.triskem-international.com/scripts/files/5c5855b887c4f4.23796223/PS_TEVA-Resin_EN_160927.pdf>

(retrieved May 6, 2020)

[50] IAEA-375 Reference Sheet, IAEA Analytical Quality Control Services, <https://nucleus.iaea.org/rpst/Documents/rs_iaea-375.pdf>

(retrieved May 6, 2020)

[51] Vajda, N.; Kim, C.-K., *J. Radioanal. Nucl. Chem.*, **2010**, *284*, 341-366.

[52] Vajda, N.; Kim, C.-K., *J. Radioanal. Nucl. Chem.*, **2010**, *283*, 203-223.

[53] Steier, P.; Dellinger, F.; Forstner, O.; Golser, R.; Knie, K.; Kutschera, W.; Priller, A.; Quinto, F.; Srncik, M.; Terrasi, F.; Vockenhuber, C.; Wallner, A.; Wallner, G.; Wild, E.M., *Nucl. Instrum. Methods Phys. Res. B*, **2010**, *268*, 1045-1049.

[54] Vockenhuber, C.; Golser, R.; Kutschera, W.; Priller, A.; Steier, P.; Winkler, S.; Liechtenstein, V., *Pramana,* **2002**, *59*, 1041-1051.

[55] Institute of Isotope Physics, University of Vienna, <https://isotopenphysik.univie.ac.at/vera> (retrieved May 6, 2020)

[56] Struminska, D. I.; Skwarzec, B., *J. Radioanal. Nucl. Chem.*, **2006**, *268*, 59-63.

[57] United Nation Scientific Committee on the Effects of Atomic Radiation, *Report to the General Assembly, with Scientific Annexes*, **2000**, *Vol. 1*.

[58] Beasley, T. M.; Kelley, J. M.; Maiti, T. C.; Bond, L. A., *J. Environmental Radioactivity*, **1998**, *38*, 133-146.

[59] Currie, L. A., *Analytical Chemistry*, **1968**, *40*, 586-593.

8 Abbreviations

Analytical methods:

AMS	accelerator mass spectrometry
A_{spike}	Spike activity [mBq]
cps	counts per second
cts	counts
LOD	limit of detection
LOQ	limit of quantification
t_{meas}	measurement time [s]

Chemical abbreviations:

Am	americium
Ar	argon
Bi	bismuth
Ca	calcium
$Ca(NO_3)_2$	calcium nitrate
CMPO	octylphenyl-*N*,*N*-diisobutyl carbamoylphosphine oxide
Co	cobalt
Cs	cesium
Eu	europium
F	fluorine
Fe	iron
Ga	gallium
Ge	germanium
$H_2C_2O_4$	oxalic acid
HCl	hydrochloric acid
He	helium
HF	hydrofluoric acid
HNO_3	nitric acid

H_2O_2	hydrogen peroxide
^{i}Bu	isobutyl
K	potassium
Na_2CO_3	sodium carbonate
$NaNO_2$	sodium nitrite
NdF_3	neodymium(III) fluoride
NH_4I	ammonium iodide
NH_4SCN	ammonium thiocyanate
$(NH_4)_2Fe(SO_4)_2$	ammonium iron(II) sulfate
Ni	nickel
NO_x	nitrogen oxides
Np	neptunium
O	oxygen
Pa	protactinium
PbF_2	lead(II) fluoride
Ph	phenyl
Pu	plutonium
Sb	antimony
Si	silicon
Sr	strontium
$TiCl_3$	titanium(III) chloride
Th	thorium
U	uranium
Zn	zinc

Others:

Å	angstrom
a	years
Ø	diameter
%	percentage

°C	degree Celsius
µg	microgram
µL	microliter
µmol	micromole
Bq	becquerel
conc.	concentrated
cm	centimeter
d	days
dest.	distilled
eq	equivalent
et al.	et alii
g	gram
h	hours
M	molar
µbar	microbar
mbar	millibar
mBq	millibecquerel
MeV	megaelectronvolt
mg	milligram
min	minute
mL	milliliter
mM	millimolar
mmol	millimole
nm	nanometer
p	pressure
PET	positron emission tomography
rpm	revolutions per minute
w	weight
w%	percentage by weight
Z	atomic number

9 Appendix

9.1 Preparation of chemicals used

Concentrated acids and other chemicals used (salts, etc.) without dilution were purchased from Sigma Aldrich, VWR or Fluka and used without further treatment.

Ion exchange resins: All ion exchange resins (Dowex, TEVA, TRU) were soaked in H_2O dest. for several hours, filtered off, and washed with the corresponding acid in a separate flask for further use and storage.

7.2 M HNO_3: HNO_3 conc. (> 65 w%) was diluted with the same amount of H_2O dest.

2 M HNO_3: 28 mL HNO_3 conc. were added to 172 mL H_2O dest. to give 200 mL 2 M HNO_3.

1 M HNO_3: 14 mL HNO_3 conc. were added to 186 mL H_2O dest. to give 200 mL 1 M HNO_3.

10 M HCl: 150 mL HCl conc. (> 37 w%; ~ 12 M) were added to 30 mL H_2O dest. to give 180 mL 10 M HCl.

9 M HCl: 120 mL HCl conc were added to 40 mL H_2O dest. to give 160 mL 9 M HCl.

8 M HCl: 100 mL HCl conc. were added to 50 mL H_2O dest. to give 150 mL 8 M HCl.

4 M HCl: 10 mL HCl conc. were added to 20 mL H_2O dest. to give 30 mL 4 M HCl.

1 M HCl: 8.2 mL HCl conc. were added to H_2O dest. in a graduated flask and the flask was filled up with H_2O dest. to the calibration mark.

0.1 M NH_4I in 9 M HCl: NH_4I (725 mg, 5 mmol) was weighed into a beaker and 38 mL H_2O dest. were added. Addition of 12 mL HCl conc. gave 50 mL 0.1 M NH_4I in 9 M HCl.

0.1 M HCl + 0.1 M HF: 2 mL HCl conc. and 1 mL HF (> 40 w%, ~ 22.7 M) were added to 247 mL H_2O dest. to give 250 mL 0.1 M HCl + 0.1 M HF.

0.05 M HCl + 0.05 M HF: Prepared *via* 1:1 dilution from 0.1 M HCl + 0.1 M HF with H_2O dest.

0.2 M $Ca(NO_3)_2$-solution: Calcium nitrate tetrahydrate (9.446 g, 40 mmol) was dissolved in 197 mL H_2O dest. to give 200 mL 0.2 M $Ca(NO_3)_2$-solution.

9.2 Spectroscopic data

9.2.1 *Cryo. 1* – data

Table 12: Alpha spectrometry data for all *Cryo. 1* samples. Note: L = leaching, F= fusion, SF = standard fusion.

Sample	m_{sample} [g]	Nuclide	Integral	s (1σ)	$t_{counting}$ [s]	Efficiency	Error	A_{spike} [mBq]	c_A [Bq/kg]	s (1σ)	Yield [%]
K1_2 + 10 µL ^{242}Pu-spike	0,095 F	Pu-242	739	27	432000	0.346	0.036	5.0			34
		Pu-239+240	446	21	432000				91.5	5.5	
		Pu-238	543	23	432000				111.4	6.3	
K1_3 + 10 µL ^{242}Pu-spike + 10 µL ^{243}Am-spike	0.196 SF	Pu-242	666	26	192000	0.346	0.036	10.0			70
		Pu-239+240	30	5	192000				3.3	0.6	
		Pu-238	13	4	192000				1.43	0.40	
		Am-243	2138	46	192000	0.346	0.036	32.2			70
		Am-241	36	6	192000				4.0	0.7	
		Th-232	989	31	508000	0.345	0.059		42.7	7.4	*see K7_5

9.2.2 *Cryo. 3* – data

Table 13: Alpha spectrometry data for all *Cryo. 3* samples. Note: L = leaching, F= fusion, SF = standard fusion.

Sample	m_{sample} [g]	Nuclide	Integral	s (1σ)	$t_{counting}$ [s]	Efficiency	Error	A_{spike} [mBq]	c_A [Bq/kg]	s (1σ)	Yield [%]
K3_2 + 10 µL ^{242}Pu-spike	0.104 F	Pu-242	758	28	504000	0.345	0.059	4.4			30
		Pu-239+240	2065	45	504000				377.2	15.9	
K3_3 + 10 µL ^{242}Pu-spike + 10 µL ^{243}Am-spike	0.116 SF	Pu-242	2669	52	800000	0.346	0.036	9.6			67
		Pu-239+240	3129	56	800000				145.5	3.8	
		Pu-238	355	19	800000				16.51	0.93	
		Am-243	10041	100	783000	0.284	0.037	45.2			98
		Am-241	1609	40	783000				64	1.7	
		Th-232	444	21	460000	0.336	0.035		36.8	4.4	*see K7_5
K3_5 + 10 µL ^{242}Pu-spike	0.100 SF	Pu-242	1861	43	605390	0.346	0.036	8.9			62
		Pu-239+240	1711	41	605390				132.2	4.4	
		Pu-238	79	9	605390				6.11	0.70	
K3_6 + 10 µL ^{242}Pu-spike	0.108 SF	Pu-242	2175	47	605380	0.284	0.037	12.7			88
		Pu-239+240	2039	45	605380				125	3.9	
		Pu-238	83	9	605380				5.09	0.57	

9.2.3 *Cryo. 7* – data

Table 14: Alpha spectrometry data for all *Cryo. 7* samples. Note: L = leaching, F= fusion, SF = standard fusion.

Sample	m_{sample} [g]	Nuclide	Integral	s (1σ)	$t_{counting}$ [s]	Efficiency	Error	A_{spike} [mBq]	c_A [Bq/kg]	s (1σ)	Yield [%]
K7_1 + 10 µL ^{242}Pu-spike	0.349 L	Pu-242	473	22	411000	0.346	0.036	3.3			23
		Pu-239+240	164	13	411000				14.3	1.3	
		Pu-238	23	5	411000				2.01	0.43	
K7_2 + 10 µL ^{242}Pu-spike	0.097 F	Pu-242	1901	44	669000	0.284	0.037	10			69
		Pu-239+240	520	23	669000				40.6	2.0	
K7_3 + 10 µL ^{242}Pu-spike + 10 µL ^{243}Am-spike	0.104 SF	Pu-242	2269	48	670000	0.346	0.036	9.8			68
		Pu-239+240	374	19	670000				22.8	1.3	
		Pu-238	93	10	670000				5.68	0.60	
		Am-243	5026	71	410000	0.284	0.037	43.2			93
		Am-241	84	9	410000				7.4	0.8	
		Th-228	250	16	258000	0.336	0.035				*see K7_5
		Th-232	229	15	258000	0.336	0.035		37.6	4.8	*see K7_5
K7_5 + 10 µL ^{232}U-spike	0.095 SF	Th-228	1942	44	421000	0.336	0.035	11.5			67
		Th-232	291	17	421000	0.336	0.035		32.1	4.0	
K7_6 + 10 µL ^{232}U-spike	0.098 SF	U-232	2884	54	590000	0.345	0.059	14.2			83
		U-238	636	25	590000				38.2	1.7	
		U-234	590	24	590000				35.5	1.6	
K7_7 + 10 µL ^{242}Pu-spike	0.104 SF	Pu-242	963	31	260000	0.346	0.036	10.7			74
		Pu-239+240	47	7	260000				6.8	1.0	
		Pu-238	13	4	260000				1.87	0.52	
K7_8 + 10 µL ^{242}Pu-spike	0.100 SF	Pu-242	830	29	260000	0.284	0.037	11.2			78
		Pu-239+240	46	7	260000				8.0	1.2	
		Pu-238	9	3	260000				1.56	0.52	

9.2.4 *Cryo. 9* – data

Table 15: Alpha spectrometry data for all *Cryo. 9* samples. Note: L = leaching, F= fusion, SF = standard fusion.

Sample	m_{sample} [g]	Nuclide	Integral	s (1σ)	$t_{counting}$ [s]	Efficiency	Error	A_{spike} [mBq]	c_A [Bq/kg]	s (1σ)	Yield [%]
K9_1 + 10 µL ^{242}Pu-spike	0.303 L	Pu-242	1213	35	411000	0.284	0.037	10.4			72
		Pu-239+240	3417	58	411000				133.9	4.5	
		Pu-238	91	10	411000				3.57	0.39	
K9_2 + 10 µL ^{242}Pu-spike + 10 µL ^{243}Am-spike	0.104 SF	Pu-242	1469	38	415000	0.336	0.035	10.5			73
		Pu-239+240	1296	36	415000				122.2	4.7	
		Pu-238	89	9	415000				8.39	0.92	
		Am-243	3143	56	260000	0.284	0.037	42.6			92
		Am-241	398	20	260000				56.4	3.0	
		Th-232	360	19	415000	0.345	0.059		35.8	6.4	*see K7_5
K9_4 + 10 µL ^{242}Pu-spike	0.101 SF	Pu-242	2510	50	800000	0.345	0.059	9.1			63
		Pu-239+240	1798	42	800000				102.1	3.2	
		Pu-238	77	9	800000				4.37	0.51	
K9_5 + 10 µL ^{242}Pu-spike	0.111 SF	Pu-242	1175	34	260000	0.336	0.035	13.5			93
		Pu-239+240	1105	33	260000				122	5.1	
		Pu-238	41	6	260000				4.53	0.72	
K9_6 + 10 µL ^{242}Pu-spike	0.098 SF	Pu-242	1113	33	260000	0.345	0.059	12.4			86
		Pu-239+240	918	30	260000				121.2	5.4	
		Pu-238	39	6	260000				5.15	0.84	

9.2.5 Reference material – data

Table 16: Alpha spectrometry data for all IAEA-375 reference material samples. Note: L = leaching, F= fusion, SF = standard fusion.

Sample	m_{sample} [g]	Nuclide	Integral	s (1σ)	$t_{counting}$ [s]	Efficiency	Error	A_{spike} [mBq]	c_A [Bq/kg]	s (1σ)	Yield [%]
Ref_1_1 + 10 µL ^{242}Pu-spike + 10 µL ^{243}Am-spike	20.330 L	Pu-242	1400	37	414800	0.345	0.059	9.8			68
		Pu-239+240	698	26	414800				0.35	0.02	
		Pu-238	150	12	414800				0.076	0.007	
		Am-243	5976	77	427800	0.336	0.035	41.6			90
		Am-241	837	29	427800				0.32	0.01	
		Th-232	819	29	12300	0.345	0.059		10.8	1.9	*Ref_3_1
		Th-228	841	29	12300	0.345	0.059		11.1	1.9	*Ref_3_1
Ref_1_2 + 10 µL ^{242}Pu-spike + 10 µL ^{243}Am-spike	10.230 L	Pu-242	1391	37	346000	0.284	0.037	14.2			98
		Pu-239+240	360	19	346000				0.36	0.02	
		Pu-238	79	9	346000				0.080	0.009	
		Am-243	4469	67	346000	0.346	0.036	37.3			81
		Am-241	542	23	346000				0.55	0.02	
		Th-232	3136	56	85000	0.346	0.036		11.9	1.3	*Ref_3_1
		Th-228	3215	57	85000	0.346	0.036		12.2	1.3	*Ref_3_1
Ref_2_2 + 10 µL ^{232}U-spike	5.067 L	U-232	2402	49	606360	0.345	0.059	11.5			68
		U-238	10243	101	606360				14.3	0.3	
		U-234	10652	103	606360				14.8	0.3	
Ref_2_3 + 10 µL ^{232}U-spike	4.906 L	U-232	429	21	107000	0.346	0.036	11.6			68
		U-238	1688	41	107000				13.6	0.7	
		U-234	1722	41	107000				13.9	0.7	
Ref_3_1 + 10 µL ^{232}U-spike	5.455 L	Th-232	1619	40	81000	0.346	0.036		12.1	1.3	
		Th-228	2079	46	81000	0.346	0.036	14.9			88

9.2.6 Blanks – data

Table 17: Alpha spectrometry data for all blank samples. Note: all samples were processed using standard fusion method.

Sample	Nuclide	Integral	s (1σ)	$t_{counting}$ [s]	Efficiency	Error	$A_{nuclide}$ [mBq]	s (1σ)
Blank_1	Pu-242	22	5	600000	0.346	0.036	0.11	0.03
	Pu-239+240	99	10	600000	0.346	0.036	0.48	0.07
	Pu-238	94	10	600000	0.346	0.036	0.45	0.07
	Am-243	7	3	431570	0.346	0.036	0.047	0.018
	Am-241	7	3	431570	0.346	0.036	0.047	0.018
	Th-232	46	7	600000	0.336	0.035	0.23	0.04
	Th-228	48	7	600000	0.336	0.035	0.24	0.04
Blank_2	Pu-242	42	6	600000	0.345	0.059	0.20	0.05
	Pu-239+240	13	4	600000	0.345	0.059	0.06	0.02
	Pu-238	11	3	600000	0.345	0.059	0.05	0.02
	Am-243	19	4	432000	0.284	0.037	0.101	0.032
	Am-241	11	3	432000	0.284	0.037	0.068	0.025
	Th-232	32	6	600000	0.284	0.037	0.21	0.04
	Th-228	27	5	600000	0.284	0.037	0.20	0.04
Blank_3	U-232	21	5	342000	0.345	0.059	0.18	0.05
	U-238	5	3	342000	0.345	0.059	0.04	0.02
	U-234	9	2	342000	0.345	0.059	0.08	0.03
Blank_4	U-232	11	3	350000	0.346	0.036	0.09	0.03
	U-238	5	2	350000	0.346	0.036	0.04	0.02
	U-234	8	3	350000	0.346	0.036	0.07	0.02

9.4 List of samples for VERA AMS-measurements

In order to quantify ^{237}Np, AMS samples were prepared from the alpha spectrometry neptunium-fraction samples (cryoconite samples and blanks), where no spikes had been added during sample preparation. The list is given in Table 18.

Table 18: List of alpha spectrometry samples used for the preparation of AMS samples at the Institute of Isotope Physics, University of Vienna.

Sample	Sample number	Fraction	Name
Blank	Blank_1	Np	Np_Blank_1
Blank	Blank_2	Np	Np_Blank_2
Cryo. 3	K3_4	Np	Np_K3_4
Cryo. 9	K9_3	Np	Np_K9_3

9.4 Abstract

Anthropogenic radionuclides have been released en masse into the environment *via* nuclear weapon tests or other incidents over the last two centuries. After transportation through the atmosphere (attached to aerosols or dust particles), these radionuclides can deposit on glaciers. Together with natural radionuclides, organic and inorganic dust, as well as microorganisms, they form so-called cryoconites. These supraglacial, highly homogenous sediments are often found in cryoconite holes and are almost 'pure' radioactive fallout, due to the lack of dilution with other matrices. As a result, very high activity concentrations of anthropogenic radionuclides can be found in cryoconites.

Identified radionuclides in cryoconite samples from Austrian glaciers in this study were ^{241}Am, ^{238}Pu, $^{239+240}$Pu, ^{232}Th, ^{238}U, ^{234}U, and ^{237}Np, with a primary focus on plutonium and americium. Different from previous studies, a new sample digestion procedure (thermal fusion with sodium carbonate) and ion exchange procedure (for separate neptunium fractions) was applied. The altered ion exchange chromatography protocol was then evaluated using a reference material. Alpha spectrometry samples of the neptunium fractions (cryoconite samples and blanks) were reprocessed for the measurement with accelerator mass spectrometry, as alpha spectrometry was not sensitive enough for interpretation.

^{241}Am activity concentrations varied from 4.1 to 65.3 Bq/kg, $^{239+240}$Pu activity concentrations ranged from 3.3 to 134.4 Bq/kg. Together with ^{232}Th (35 – 43 Bq/kg), the observed activity concentrations were in good correspondence with previously published data, indicating a good suitability of the newly applied procedures.

9.5 Zusammenfassung

Im Laufe der letzten beiden Jahrhunderte wurde durch den Menschen eine große Menge an Radionukliden in die Umwelt freigesetzt, zum Beispiel durch Kernwaffentests und diverse Unglücksfälle. Sobald sie freigesetzt werden, haften sich diese Radionuklide an Aerosole oder Staubpartikel und werden in weiterer Folge in der Atmosphäre verteilt, bis sie sich schließlich auf Oberflächen ablagern. Auf Gletschern entstehen gemeinsam mit anderen, natürlichen Radionukliden, organischen und anorganischen Staubpartikeln, oder auch Mikroorganismen, sogenannte Kryokonite. Diese besonders homogenen Sedimente findet man oft in Kryokonitlöchern und sie bestehen aus praktisch komplett reinem Fallout, da es zu so gut wie keinen Mischprozessen mit anderen Matrizes kommt. Aus diesem Grund können in Kryokoniten besonders hohe Aktivitätskonzentrationen von anthropogenen Radionukliden nachgewiesen werden.

In dieser Arbeit wurden Kryokonitproben von österreichischen Gletschern bearbeitet und darin folgende Radionuklide untersucht: ^{241}Am, ^{238}Pu, $^{239+240}$Pu, ^{232}Th, ^{238}U, ^{234}U und ^{237}Np. Das Hauptaugenmerk wurde dabei auf Americium und die Plutonium-Isotope gelegt. Zur Anwendung kamen dabei eine neue Probenaufschlussmethode (Schmelzaufschluss mit Natriumcarbonat), sowie ein neues Ionenaustauschchromatographie-Protokoll (um eine separate Neptunium-Fraktion zu erhalten). Diese Ionenaustauschchromatographie-Methode wurde anschließend mithilfe eines Referenzmaterials auf deren Eignung überprüft. Da eine Auswertung der bereits mit Alpha-Spektrometrie vermessenen Proben der Neptunium-Fraktionen (Kryokonitproben und Blanks) nicht möglich war, wurden diese anschließend erneut aufbereitet, um diese in weiterer Folge mittels Beschleuniger-Massenspektrometrie zu analysieren, welche eine wesentlich empfindlichere Messmethode ist.

Die gemessenen ^{241}Am-Aktivitätskonzentrationen lagen in einem Bereich von 4,1 bis 65,3 Bq/kg, die von $^{239+240}$Pu zwischen 3,3 und 134,4 Bq/kg. Zusammen mit den Konzentrationswerten von ^{232}Th (35 bis 43 Bq/kg) lässt sich sagen, dass sich die Werte in guter Übereinstimmung mit den für diese Proben bereits publizierten Daten befinden. Dies lässt den möglichen Schluss zu, dass die erwähnten, neu angewendeten Methoden sich gut für die Bestimmung von Radionukliden in Kryokoniten eignen.